**EFFECTS OF THINNING ON CARBON DYNAMICS
IN A TEMPERATE CONIFEROUS FOREST**

By
Janelle S. Trant, B.Sc.[Env]

A Thesis
Submitted to the School of Graduate Studies
In Partial Fulfillment of the Requirements
For the Degree
Master of Science

McMaster University

MASTER OF SCIENCE (2013)   **MCMASTER UNIVERSITY**

(EARTH SCIENCES)   **HAMILTON, ON**

TITLE**:** Effects of thinning on carbon dynamics in a temperate coniferous forest

AUTHOR: Janelle S. Trant, B.Sc.[Env] (University of Guelph)

SUPERVISOR: Dr. M. Altaf Arain

NUMBER OF PAGES: ix, 63

ABSTRACT

Forest ecosystems are a significant component of the global carbon (C) cycle. Afforestation is considered a cost-effective and ecologically viable means to sequester atmospheric carbon. However, afforestation requires intensive management practices, including thinning, to maintain and enhance the carbon sequestration capability of the forest. This study examines thinning effects on forest carbon dynamics using eddy covariance (EC) methods. In January 2012, a 74-year-old white pine (*Pinus strobus*) plantation located in southern Ontario was selectively thinned. Approximately 30% of trees, equating to 2308 m^3 of wood (sawlogs and pulpwood), were removed to improve light, water and nutrient availability for remaining trees. Fluxes of energy, water, carbon dioxide (CO_2) as well as meteorological variables were measured throughout the year following thinning and compared to data from the previous 9 years to evaluate effects of thinning on forest carbon dynamics. Mean annual net ecosystem productivity (NEP), gross ecosystem productivity (GEP) and ecosystem respiration (RE) from the 9 years prior to thinning were 290, 1413 and 1118 g C m^{-2}, respectively. Post-thinning NEP, GEP and RE were 154, 1509 and 1350 g C m^{-2} year^{-1}, respectively. Post-thinning NEP was significantly less than pre-thinning at the annual time scale due to higher RE, however post-thinning fluxes were still within the range of interannual variability. At this site, approximately 20% of interannual variability in NEP, GEP and RE was explained by environmental conditions. Effects of extreme weather events, particularly heat and drought stress, were demonstrated to negatively impact NEP. Biotic responses to environmental drivers explained the remaining 80% of interannual variability in fluxes. Thinning did not significantly impact these responses. Further, results suggest that thinning may improve tolerance to drought stress by improving water availability for remaining trees. Therefore, thinning has the potential to effectively reduce resource competition and stimulate growth and carbon sequestration in temperate coniferous forests.

ACKNOWLEDGEMENTS

TABLE OF CONTENTS

LIST OF FIGURES

LIST OF TABLES

SYMBOLS AND ABBREVIATIONS

BA	basal area	(m^2 ha^{-1})
BHI	Beaumont Heat Index	
C	carbon	
CO_2	carbon dioxide	
EC	eddy covariance	
ET	evapotranspiration	(mm)
GCM	global climate model	
GEP	gross ecosystem productivity	(g C m^{-2} $year^{-1}$)
LAI	leaf area index	(m^2 m^{-2})
NEE	net ecosystem exchange	(g C m^{-2} $year^{-1}$)
NEP	net ecosystem productivity	(g C m^{-2} $year^{-1}$)
OMNR	Ontario Ministry of Natural Resources	
P	precipitation (rain and snow)	(mm)
PAR	photosynthetically active radiation	(μmol m^{-2} s^{-1})
PDSI	Palmer Drought Severity Index	
PPFD	downward photosynthetic photon flux density	(μmol m^{-2} s^{-1})
RE	ecosystem respiration	(g C m^{-2} $year^{-1}$)
RH	relative humidity	(%)
SI	site index	
SI_{25}	site index at base age 25 years	
SD	standard deviation	
SM	soil moisture	
Ta	air temperature	(°C)
Ts	soil temperature	(°C)
TPD	80-year-old naturally-regenerated deciduous stand	
TPFS	Turkey Point Flux Station	
TP39	74-year-old white pine plantation	
TP74	39-year-old white pine plantation	
VPD	vapor pressure deficit	(kPa)
VWC	volumetric water content	(m^3 m^{-3})
WUE	water use efficiency	(g C kg^{-1} H_2O)

CHAPTER 1: INTRODUCTION

Forest ecosystems cover approximately 30% of Earth's total land area, and represent a significant carbon (C) sink (2.4 ± 0.4 Pg C year^{-1} over 1990-2007) in the global cycle (Dixon et al. 1994; Pan et al. 2011). The largest global carbon dioxide (CO_2) flux is terrestrial gross ecosystem productivity (GEP), 47% of which is from forest biomes (i.e. 59 Pg C year^{-1}) (Beer et al. 2010). Forests support numerous vital ecosystem services, and influence climate through exchanges of water, carbon, energy and nutrients (Raffaelli and Frid 2010; Bonan 2008). Many global climate models (GCMs) forecast significant changes to the world's climate over the next century (Field et al. 2012). Warmer surface temperatures, intensified precipitation events followed by extended periods of drought, increased atmospheric CO_2 concentrations and more frequent and severe extreme weather events are examples of changes likely to have significant impacts on forest ecosystems (Field et al. 2012). Such changes are predicted to affect species ranges, disturbance frequency and intensity, and productivity of global forest ecosystems (Field et al. 2012; Ledig and Kitzmiller 1992; Hansen et al. 2001; Granier et al. 2007; Holst et al. 2008).

The significant role of forests in the global carbon cycle has led to interest in managing forests for climate change mitigation. This primarily involves maximizing forest carbon uptake and long-term storage (Dixon et al. 1994; D'Amato et al. 2011). Afforestation, the establishment of forests on previously unforested land, is considered one cost-effective and ecologically viable means to sequester atmospheric carbon. However, for afforestation practices to be successful, intensive stand management is required. Common forest management practices include site preparation, selection of species and genotypes,

planting, fertilization, prescribed burning, weed control and thinning (Bettinger et al.

2009). Thinning, the removal of a substantial number of trees from a stand, is a common

practice intended to reduce resource competition and stimulate growth and carbon

sequestration for remaining trees that may have been constrained by the availability of

light, water and nutrients (Smith et al. 1997; Spittlehouse and Stewart 2003). In Ontario,

two silvicultural systems are applied for thinning: shelterwood and selection (Ontario

Ministry of Natural Resources [OMNR] 2011b). Methods of thinning applied in other

regions include low, crown, selection and geometric (Smith et al. 1997). In most instances,

approximately 30% of the original stand is harvested (Spittlehouse and Stewart 2003). In

the past, the most common objective of thinning was timber production. However, in

recent years carbon sequestration and forest conservation have also become important

management goals. It is important to understand and quantify impacts of thinning on forest

carbon dynamics, particularly if stand management objectives include carbon

sequestration.

Eddy covariance (EC) is a well-established method for measuring carbon, water and

energy fluxes between land surfaces (e.g. forests) and the atmosphere (Baldocchi et al.

2001; Baldocchi 2008). Applications of these measurements include long-term monitoring,

inter-site comparisons and climate model calibration, among others (Gower et al. 2001).

Globally, there are over 400 active research sites currently using EC techniques to measure

fluxes over a range ecosystems (Baldocchi et al. 2001; Baldocchi 2008; Fluxnet 2013).

Several studies conducted at these sites have evaluated effects of prescribed thinning

operations on carbon and water exchanges in forest ecosystems varying in age, geographic

location, climate and dominant species (Saunders et al. 2012; Scott et al. 2004; Dore et al.

2012; 2010; Vesala 2005). In coniferous forests, results of thinning on carbon and water

exchanges measured by EC techniques have varied. Several studies have reported minor

effects of thinning on carbon uptake in coniferous forests, with recovery of the thinning-

depleted carbon sink within a couple of years (Vesala et al. 2005; Dore et al. 2010; 2012;

Saunders et al. 2012). Saunders et al. (2012) reported that thinning of a temperate old-

growth Sitka spruce forest in Ireland did not have a significant effect on rates of carbon

sequestration, but that it did increase the interannual variability in net ecosystem exchange

(NEE; negative values indicate carbon uptake by forest). Other studies have reported

longer recovery times for depleted carbon sinks following thinning, such as Scott et al.

(2004) who predicted that it would take five years for a boreal Scots pine forest to re-

sequester the carbon lost during the thinning operation. Several studies have also

investigated the re-allocation of carbon sources and sinks following thinning. Furthermore,

the importance of considering and accounting for understory growth following thinning

has been highlighted by Vesala et al. (2005), Campbell et al. (2009) and Moreaux et al.

(2011).

Research has also demonstrated connections between climate variability and

thinning effects. Influences of climate variations, particularly air temperature (Ta),

precipitation (P) and photosynthetically active radiation (PAR) have been shown to alter

the expected impacts of thinning in a temperate old-growth Sitka spruce forest (Saunders

et al. 2012). Further, a long-term study in a southern ponderosa pine forest in Arizona, USA

found that following thinning, more carbon was stored during dry months compared to wet

months, suggesting improved drought tolerance (Dore et al. 2010). Several years later, a continuation of this study found evidence of improved heat tolerance as shown by a higher Ta at maximum GEP compared to previous observations (Dore et al. 2012). These findings are especially important because heat and drought stress are expected to become more prevalent in the future (Field et al. 2012).

There is a need for a better understanding of the effects of thinning, particularly under the shelterwood management system, on afforested and managed temperate coniferous forests (Scott et al. 2004). In Ontario, approximately 80% of the 71 million hectares (ha) of forest are provincially owned and managed (OMNR 2011a). Thinning is a common management practice; between 2000 and 2010, over 130,000 ha of managed forests were thinned (OMNR 2011a). A better understanding of the effects of thinning on such forests will provide insight into how the efficiency of thinning treatments may be altered to maximize carbon sequestration and improve the forest's tolerance to environmental stress in this region.

In this paper, we examine the impacts of forest thinning (30% removal of trees) on forest carbon dynamics during the first post-thinning year (2012) using micrometeorological methods. We compare these measurements with pre-thinning fluxes measured at this site from 2003 to 2011. In our study, 2003-2011 is referred to as the pre-thinning period, and 2012 the post-thinning period. Study objectives are to (1) evaluate effects of climatic variability and extreme weather events on forest carbon dynamics; and (2) determine the impact of thinning on canopy characteristics and carbon sequestration

4

capabilities of the stand. We hypothesize that thinning will not significantly affect GEP in the first post-thinning year, and that increases in RE will be the major cause of observed decreases in NEP.

CHAPTER 2: MATERIALS AND METHODS

2.1 Study site

This study was conducted in a 74-year-old eastern white pine (*Pinus strobus L.*) plantation forest located near the north shore of Lake Erie in southern Ontario, Canada (42◦71N, 80◦35W). Referred to in short as TP39 for the year in which it was planted, this 39 ha site is part of the Turkey Point Flux Station (TPFS), an age-sequence of stands consisting of three white pine plantations (11-, 39- and 74-years-old in 2013) and a naturally-regenerated deciduous stand (approximately 80-years-old in 2013). Like many other afforestations in the area, the OMNR established TP39 on cleared oak savannah to generate timber revenue and stabilize the highly erodible sandy soil. Species composition is 82% white pine; remaining species include oak (*Quercus velutina L., Quercus alba L.*), maple (*Acer rubrum L., Acer sachrum L.*), black cherry (*Prunus serotina Ehrh*) and balsam fir (*Abies balsamea L.*) (Peichl et al. 2006; Peichl et al. 2010a; Elliott et al. 2011). Understory vegetation includes bracken fern, poison ivy, Canadian Mayflower, allegheny raspberry and mosses (Arain and Restrepo-Coupe 2005). The 30-year mean annual Ta and P in this region are 8.0◦C and 1036 mm, respectively, over 1981-2010 (Environment Canada 2013). On an annual basis, rainfall accounts for 906 mm of the 30-year mean P, and snowfall accounts for 130 mm. Approximately 457 mm of P falls during the most productive months (May to September) of the growing season (Environment Canada 2013).

Soil at the site is classified as Brunisolic Grey Brown Luvisol (Presant and Acton 1984). It is very sandy (~98% sand, 1% silt, <1% clay), well-drained, and has a low-to-moderate water holding capacity (Peichl et al. 2010a). Topography is predominantly flat. Field capacity and wilting point are estimated to occur around soil volumetric water contents (VWC) of 0.16 $m^3 m^{-3}$ and between 0.01 and 0.04 $m^3 m^{-3}$, respectively (Peichl et al. 2010a). Plant stress is estimated to occur below 0.068 $m^3 m^{-3}$, indicated by a positive relationship between xylem sapflow velocity and VWC below this moisture content (McLaren et al. 2008; MacKay et al. 2012).

2.2 Thinning operation

TP39 is managed by the OMNR and is currently in the preparatory stage of development under the shelterwood silvicultural system (Elliott et al. 2011). This silvicultural system is characterized by two or more partial cuts (also known as thinnings) over the course of 10 to 30 years, with each cut allowing for the regeneration and development of seedlings in partial shade (OMNR 2011b). The first partial cut took place in 1983, at which time approximately 108 $m^3 ha^{-1}$ of wood volume was removed (Elliott et al. 2011). In winter 2012, the second partial cut was conducted (Elliott et al. 2011). A mechanical harvester was used to cut, de-limb and section the trees. A forwarder transported logs to a loading area at the perimeter of the forest, where they were stored for transportation to a mill near Sudbury, Ontario. To reduce soil compaction and disturbance during this operation, pre-existing multi-use trails throughout the stand were used where possible. Thinning residues (e.g., limbs, bark, crowns) were placed on the ground ahead of the harvester and forwarder to reduce compaction where trails were not accessible.

6

Approximately 200 legacy trees (largest, best quality) were retained on each hectare, and

remaining trees were harvested. In total, approximately 2308 m^3 of wood volume was

removed from this stand, equating to approximately 60 m^3 ha^{-1}. Of the total amount

harvested, 352 m^3 were pulpwood and 1958 m^3 were sawlogs (P. Kallioinen, personal

communication, June 20, 2013). Using a volume (m^3) to mass (metric tonnes, t) conversion

factor of 0.854 provided by the mill that processed the pulpwood, the total amount of wood

harvested was 1973 t (P. Kallioinen, personal communication, June 20, 2013). Peichl and

Arain (2007) used destructive methods at this site to determine the approximate allocation

of total tree biomass between above- and belowground pools: 69% stem, 1.5% foliage, 7%

living branches, 4.5% dead branches and 18% roots. Based on these proportions and the

total amount of harvested stems (i.e. 1973 t), it is estimated that at total of 2859 t of

biomass were affected by this operation in 2012. The operation added 43 t of foliage, 200 t

of live branches and 129 t of dead branches to the forest floor. An additional 515 t of roots

were made inactive from growth and production. These components, totaling 887 t of

biomass, will eventually decompose and contribute significantly to heterotrophic

respiration in coming years at this site. Stand characteristics were also greatly impacted by

the thinning operation as summarized in Table 1 (Peichl et al. 2010b; Kula 2013).

Table 1. Stand characteristics.

	2003*	2004	2005	2006	2007	2008	2009	2010	2011	2012
Basal area (m^2 ha^{-1})	N/A	37.7	37.7	38.4	38.7	39.4	40.1	40.3	40.7	35.6
Mean tree height (m)	N/A	20.3	20.8	21.3	21.8	22.5	22.7	22.8	22.8	23.2
Mean DBH (cm)	N/A	34.8	34.9	35.3	35.6	35.9	36.3	36.7	36.8	38.7

*Biometric Measurements began in 2004.

On average, basal area (BA) was reduced by 13% (from 40.7 to 35.6 m^2 ha^{-1}) (Kula

2013). Peak leaf area index (LAI) was reduced by 35% (from 8.5 to 5.5 m^2 m^{-2}) (measured

by Dr. Jing Chen's Remote Sensing and GIS group at the University of Toronto; Chen et al. 2006). Figure 1 shows photographs of an area near the flux tower prior to and after the thinning operation.

2.3 Meteorological measurements

Continuous meteorological measurements have been made at TP39 since 2003 (see Peichl et al. 2010a for additional details). Ta and relative humidity (RH) were measured at three heights: above-, mid- and below-canopy (model HMP45C, CSI). Vapor pressure deficit (VPD) was calculated from measurements of Ta and RH. Above-canopy wind speed and direction (WS, model 05 103-10RE, R.M. Young Co.), net radiation (Rn, model NR-LITE, Kipp and Zonen Ltd) and PAR (model LI-200S, LI-COR Inc.) were also measured approximately 28 m above ground at the top of a scaffolding tower located within the stand. Two spatially distinct soil pits were used to measure soil moisture (SM, model 615/616, CSI) and soil temperature (Ts, model 107B, CSI, respectively) at depths of 2, 5, 10, 20, 50 and 100 cm. Year-round P was measured in an open area at the Normandale Fish Hatchery (2 km northeast of site) using a weighted rain gauge (model T200B, Geonor Inc.). This rain gauge was relocated to Long Point Waterfowl (1.5 km east of site) in 2011. A tipping bucket rain gauge (model TE525, Texas Instruments) was installed beside the weighted rain gauge to cross-check measurements. P was also measured above the TP39 canopy (20 m above the ground) using a heated tipping bucket rain gauge (model 52202, R.M. Young Co.). Atmospheric pressure (model 61205V, R.M. Young Co.), snow depth (model SR50, CSI) and water table height (model OTT PLS, CSI) were also measured.

Gaps in metrological variables were filled using data from the three nearby TPFS sites. To fill gaps, year-long comparisons were performed between simultaneous measurements at TP39 and the three other sites. The site with the highest coefficient of determination (R^2) was used to fill the gaps in TP39 measurements using a regression. Normalization was applied to account for physiological differences between the two sites. Gaps in P measured by the weighted rain gauge were filled using measurements from the two nearby tipping bucket rain gauges. Gaps in incoming shortwave radiation (SW) were filled using a linear relationship with measured PAR. Soil heat flux was calculated by applying a correction factor to buried heat flux plate measurements (model HFT3, CSI) to include heat storage in the overlying three centimeters of soil.

To evaluate the occurrence of extremely high Ta events throughout the study period, a heat stress index following Beaumont et al. (2011) was applied (Beaumont Heat Index, BHI). This index considers months with average Ta exceeding two standard deviations (SD) from the 30-year normal as "extreme" (Beaumont et al. 2011). Monthly normals from 1981-2010 recorded at an Environment Canada weather station in Delhi, Ontario (20 km northwest of TP39) were used to determine which study period months were extremely hot (Environment Canada 2013; McLaren et al. 2008).

2.4 Eddy covariance measurements

A closed-path EC system, consisting of an infrared gas analyzer (IRGA, model LI-7000, LI-COR Inc.), sonic anemometer (model CSAT-3, CSI), climate control box, four meter long heated sampling tube and a desktop computer was used to estimate half-hourly NEE

of CO_2 (negative values indicate carbon uptake by forest) (Arain and Restrepo-Coupe 2005). A second IRGA was used to measure mid-canopy (14 m) CO_2 concentrations to calculate changes in CO_2 storage in the air column below the EC system (model LI-820, LI-COR Inc.). Continuous flux measurements (20 Hz) were made at the top of the tower from January 2003 to December 2012.

High-frequency EC data were saved on a desktop computer housed in a trailer near the tower. Software developed by Dr. T.A. Black's Biometeorology and Soil Physics Group at the University of British Columbia was used to calculate half-hourly fluxes. Changes in carbon storage in the air column below the EC system were calculated from the difference between corresponding above- and mid-canopy CO_2 measurements. NEE was calculated by adding the measured half-hourly flux of CO_2 (Fc) and CO_2 storage. From this, NEP was calculated as the inverse of NEE (NEP = -NEE).

Processes applied to the calculated half-hourly fluxes, in order of operation, were: (1) outlier and spike removal; (2) footprint filtering; (3) friction velocity (u_*) threshold filtering; (4) RE gap-filling; (5) partitioning of NEP into GEP; (6) GEP gap-filling; and (7) filling of NEP gaps resulting from instrument malfunction, power outages, calibration or data processing. With the exception of storage calculations, all of these processes were run separately for pre- and post-thinning periods (2003-2011 and 2012, respectively) to avoid confounding effects caused by any phenological changes in the stand resulting from thinning. Details of these processes are described in Brodeur (2013) and in Appendix A.

Differences between pre- and post-thinning annual sums of GEP, RE and NEP, as well as annual GDD and P, were evaluated using t-tests in MATLAB (The Mathworks Inc).

2.5 Uncertainty estimates associated with EC measurements

There are numerous sources of uncertainty associated with EC methods. Uncertainty may result from errors associated with the operator, population sampling, instruments, calibration and measurement conditions (Aubinet et al. 2012). These errors may be random or systematic. Random errors are unpredictable errors that result in scattered data, while systematic errors are constant yet unknown (Aubinet et al. 2012). Random errors in flux measurements may be caused by the nature of turbulence and resulting sampling errors, random measurement errors, and changes in the footprint (Aubinet et al. 2012). Systematic errors arise when the EC assumptions are not met, and from calibration and processing problems (Aubinet et al. 2012). On ideal sites, it is estimated that uncertainty in annual NEP is less than 50 g C m^{-2} (Baldocchi 2003). A previous study conducted at this site estimated that between 2003-2007, average uncertainty in annual NEP was ±40 g C m^{-2} year^{-1} based on half-hourly mean absolute error (MAE) (Peichl et al. 2010a).

2.6 Comparison with nearby forest sites

Carbon dynamics from an adjacent 39-year-old white pine plantation forest (TP74, Peichl et al. 2010a) and an 80-year-old deciduous forest (TPD, Parsaud 2013) located 20 km west of the thinned stand (TP39) were compared to TP39. Because the EC system at TPD was established in early 2012, and coniferous and deciduous forests are different with

11

respect to physiological characteristics and carbon sequestration strategies, this comparison focused mainly on TP74.

In 2012, average tree height, average diameter at breast height (DBH) and LAI at TP74 were 16 m, 18 cm and 6.6 m^2 m^{-2}, respectively. Located adjacent to TP39 on the south side, TP74 was selected as a control comparison for TP39 because it was not thinned, it is relatively similar in age to TP39 and it experienced identical meteorological conditions. EC and meteorological measurements have been made at this site since 2003. A roving open-path EC system (comprised of Li-7500 IGRA and CSAT3 sonic anemometer) was used from 2003-2007 on top of a 16 m tower. In 2008, a 20 m scaffolding tower was erected and the EC system was upgraded to a permanent closed-path system (Peichl et al. 2010a). Because of differences between the open- and closed-path systems (e.g. different measurement heights) and uncertainty resulting from filling large data gaps prior to 2008, only measurements from the permanent closed-path system were considered in this analysis (i.e. from 2008 to 2012).

The closed-path system at TP74 consisted of an infrared gas analyzer (IRGA, model LI-7000, LI-COR Inc.), sonic anemometer (model CSAT-3, CSI), climate control box, heated sampling tube and a desktop computer. Key meteorological variables (Ta, Ts, VWC, RH, PAR) were also measured. Outlier and spike removal, u_* threshold filtering and gapfilling processes were identical at both sites. A footprint filter was not applied at TP74 because it was not critical to exclude fluxes from surrounding stands since this site was not thinned.

To account for age-related differences between TP39 and TP74, carbon fluxes were normalized based on a standard forestry measure of site quality (site index, SI). Previous work at the TPFS determined site-specific SI values based on tree height measurements and stand age, using standard eastern white pine relationships between dominant tree height and base age 25 (i.e. SI_{25} curves) (Peichl et al. 2010a; Parresol and Vissage 1998). SI values determined by Peichl et al. (2010a) were used in this analysis. Site indices at TP39 and TP74 were 7.9 and 8.4, respectively (Peichl et al. 2010a). Site-specific normalization factors were computed by dividing the reference SI_{25} at TP39 by the SI_{25} at TP39 and TP74, resulting in normalization factors of 1 and 0.93, respectively. Carbon fluxes were multiplied by these site-specific normalization factors.

2.7 Determination of functional relationships

Functional relationships between measurements of productivity (in this case unfilled NEP), and key meteorological variables (Ta, PAR, VPD and VWC) were examined to evaluate possible thinning effects. NEP was chosen to represent productivity instead of GEP because the latter is entirely modeled. Unfilled NEP was used to further reduce potential errors associated with the gap-filling process. Only daytime growing season measurements (April 1- October 31) were considered. Once daytime growing season measurements were selected, NEP was bin-averaged using bin sizes of 50 μmol m^{-2} second^{-1} for PAR, 0.5°C for Ta, 0.05 kPa for VPD and 0.05 m^3 m^{-3} for VWC. A moving average was calculated for each year to show the general trend of each annual relationship.

2.8 Crossed- meteorological and parameter year test

A simplified test following Richardson et al. (2007) was performed to partition fluxes into two main effects: variation in environmental drivers and variation in biotic responses to environmental forcing. Environmental drivers included: Ta, Ts at 5 cm depth, PAR, VPD and VWC. Gapfilling model parameters, or coefficients, were used to characterize biotic responses to environmental forcing. Richardson et al. (2007) predicted that changes in the biotic response to environmental forcing might be caused by differences in maximum process rates (e.g., maximum GEP), sensitivity of key processes to environmental drivers (e.g., response of RE to Ta) and changes in the size or distribution of the carbon pool.

Model coefficients for GEP and RE, parameterized and used during the gap-filling process to estimate half-hourly carbon fluxes based on corresponding observations of meteorological conditions, were derived for each year during the gapfilling process. For each year between 2003-2012, GEP and RE were modeled by crossing each 'meteorological year' (i.e. each of the 10 years of meteorological data) with each 'parameter year' (i.e. each of the 10 years of model parameter sets), resulting in 100 different combinations for each flux component. For each combination of 'meteorological year' and 'parameter year', NEP was calculated as the difference between the estimates of GEP and RE. A two-way analysis of variance (ANOVA) was performed in MATLAB to partition the variability in model predictions of annual fluxes into 'meteorological year' and 'parameter year' effects. The ANOVA error term accounted for the remaining unexplained variance. Multiple comparisons were used to evaluate which years exhibited meteorological and biotic conditions conducive to higher rates of GEP, RE and NEP.

CHAPTER 3: RESULTS

3.1 Climate variations throughout study period

Table 2 provides annual growing season (April 1 – October 31) climatic conditions for 2003-2012. Throughout the study period, annual mean annual Ta ranged from 7.5 to 10.3°C. Mean annual pre-thinning (2003-2011) Ta was 8.4±0.8°C, and mean annual post-thinning (2012) Ta was 10.3°C, respectively. Annual growing season Ta ranged from 14.1 to 16.6°C. Highest annual growing season values were observed in 2005 and 2012. Monthly trends in Ta varied between years (Fig. 2a). Deviations from normal included a warm winter in 2006, a relatively cold winter in 2007, a warm summer in 2005 and an unusually warm winter and spring in 2012. On average, 2012 was the warmest year of the study period; January, February, March, June and July were warmer than in all pre-thinning years. Most remarkably, monthly average Ta in March 2012 was 7.3°C, compared to the 30-year normal (1981-2010) of 0°C (Environment Canada 2013). During the study period, three years had at least one extremely hot month during the growing season according to the BHI (Beaumont et al. 2011). In 2005, June and September were extremely hot (0.3 and 1.8 degrees warmer than 2 SD, respectively). October 2007 was 1.0 degree above 2 SD. In 2012, March and July were both extremely hot (3.5 and 0.2 degrees above 2 SD, respectively).

Mean annual PAR ranged from 311.8 to 345.2 µmol m^{-2} second^{-1} over 2003-2012. Mean annual pre- and post-thinning PAR was 327.2±12.7 and 345.2 µmol m^{-2} second^{-1}, respectively. Mean annual growing season PAR ranged from 408 to 462 µmol m^{-2} second^{-1}. Maximum and minimum annual growing season PAR were observed in 2012 and 2003,

15

respectively. Monthly mean PAR was lower than normal during March 2004 and April to May 2011, and was higher than normal during June 2007 (Fig. 2b). Periods of relatively low PAR were associated with abundant P. Upward, or reflected, PAR was also measured. Mean annual pre- and post-thinning reflected PAR was 10.0 µmol m^{-2} second^{-1} and 12.6 µmol m^{-2} second^{-1}, respectively. Mean monthly reflected PAR in 2012 was higher than pre-thinning years during May, July and August. This was a combined effect of high incoming PAR and increased exposure of bare soil and understory vegetation following the thinning operation. Bare soil and understory vegetation have a higher albedo than pine trees, increasing reflected radiation.

VPD, a function of Ta and RH, exhibited interannual variability throughout the study period. Mean annual growing season VPD ranged from 0.6 to 1.0 kPa. Mean annual growing season pre- and post-thinning VPD was 0.7±0.1 and 1.0 kPa, respectively. Low monthly values were observed in July and August 2010 and March to May 2011 (Fig. 2c). Maximum monthly VPD was higher in March, May, July, August and September of 2012 compared to pre-thinning years.

Annual P during the study period ranged from 896 to 1293 mm (Fig. 2d). Mean pre-thinning P was 960±158 mm and post-thinning P was 1001 mm. Pre- and post-thinning annual P were not significantly different (p = 0.4519). Previous work at this site evaluated the occurrence of extreme drought events using the Palmer Drought Severity Index (PDSI) (Peichl et al. 2010a). Droughts were not evident in 2003 or 2006. The 2004 growing season began with a wet spring, but a minor drought developed towards the end of the summer

16

(Peichl et al. 2010a). This mild drought was maintained until the middle of the 2005

growing season. In 2007, increasingly limited water availability throughout the growing

season resulted in an extreme drought by the end of the summer (Peichl et al. 2010a).

Highest annual rainfall was recorded in 2011, nearly half of which occurred by May. Cloudy,

rainy conditions during this period contributed to low PAR (Fig. 2b). Cumulative P in 2012

was low compared to previous years until late summer. By the end of the year, cumulative

P was average because of several large events that occurred in the fall. In 2012,

approximately 226 mm of P fell as snow, and 775 mm as rain. The rainband of Hurricane

Sandy passed through this region in late October, resulting in 62 mm of rain over 4 days.

Table 2. Annual growing season (April 1 – October 31) climatic conditions. All reported values are averages except for precipitation (P), which is an annual cumulative sum. Only daytime values were considered for vapor pressure deficit (VPD).

	2003	2004	2005	2006	2007	2008	2009	2010	2011	2012
Ta (°C)	14.1	14.5	16.6	15.6	15.6	14.6	14.1	15.9	15.3	16.2
Ts (°C)	13.8	14.0	14.4	14.2	14.3	13.4	13.2	14.7	14.3	14.9
P (mm)	583	492	477	752	441	508	608	608	745	650
PAR (μmol m^{-2} s^{-1})	408	418	458	411	459	451	437	439	417	462
VPD (kPa)	0.64	0.56	0.75	0.76	0.83	0.61	0.55	0.61	0.69	1.02
VWC (m^3 m^{-3})	0.11	0.11	0.10	0.12	0.09	0.12	0.11	0.10	0.11	0.09

SM, a function of P, soil texture and soil structure, is an important secondary

controlling factor for GEP and RE (Richardson et al. 2007). Previous research conducted at

this site identified that below a VWC threshold of 0.068 m^3 m^{-3}, trees experience water

stress (McLaren et al. 2008; MacKay et al. 2012). To evaluate the annual extent of water

stress, days with average VWC below this threshold were identified. Years with the most

frequent number of water stress days were 2007, 2011 and 2012. In 2007 there were 70

days with average daily VWC below 0.068 m3 m^{-3}. This corresponds with the growing

season-long drought identified by the PDSI in 2007 (Peichl et al. 2010a). The last two years of the study period were very similar; 2011 and 2012 had 50 and 54 water stress days, respectively. In 2011, this was driven by limited P between May and August, whereas there was limited P until late August in 2012.

Annual growing degree days (GDD), a measure of heat accumulation over the growing season, ranged from 1137 to 1621°D between 2003-2012 (Fig. 3). Mean pre-thinning GDD was 1354±159°D; GDD in the post-thinning year was 1562°D. Pre-thinning GDD was significantly less than post-thinning (p = 0.0044). The year with the lowest GDD was 2009; relatively low growing season Ta was observed in this year (Fig. 2a). Compared to previous years, 2012 maintained the highest GDD for the majority of the growing season, particularly between June and August. This high rate of GDD accumulation corresponds with the extremely hot Ta in July identified by the BHI. In mid-September, GDD in 2005 surpassed that of 2012 (Fig. 3). September 2005 was also identified as extremely hot by the BHI.

3.2 Carbon and water dynamics throughout study period

Figure 4 shows half-hourly non-gap-filled measurements of NEP throughout the study period. Positive daytime values represent photosynthetic carbon uptake via GEP; negative values represent carbon losses due to RE. All years show the same general trend of dormancy in the winter followed by long, productive growing seasons. A mid-summer decline in productivity was observed in 2005 and to a greater extent in 2011 and 2012. In all instances, these declines were followed by a recovery to normal values.

18

Figure 5 demonstrates the modeled response of RE to changes in Ts, using coefficients derived from the gap-filling process (coefficients are given in Appendix B). For all possible soil temperature values, 2012 exhibited one of the highest rates of respiration, along with 2003, 2004 and 2008. Overall, however, the relationship between modeled RE and Ts was not significantly different. The modeled response of GEP to changes in PAR, using coefficients derived from the gap-filling process (coefficients are given in Appendix B), also demonstrates no substantial effect of thinning (Figure 6). Again, the response in 2012 was within the range of interannual variability. Years 2008 and 2010 demonstrated the highest rates of GEP with increasing PAR; 2006 demonstrated the lowest.

Figure 7 shows monthly dynamics of GEP and RE. The early growing season start in 2012 is apparent in the remarkably high dynamics of GEP and RE in March. Maximum monthly GEP was observed in July 2008. March 2012, June 2010 and July 2010 also demonstrated relatively high monthly GEP. Conversely, the year with the lowest GEP throughout the majority of the growing season was 2005. Maxiumum monthly RE was observed in August 2003. Relative to other years, monthly RE was low in 2011 for most of the growing season. Although monthly dynamics of GEP were very similar in 2011 and 2012, RE was higher in 2012 compared to 2011. The mid-summer decline in productivity in 2011 and 2012 is visible in the monthly dynamics of GEP (Fig. 7). GEP typically reaches an annual maximum in July at this site, however this was not observed in 2011 and 2012. Instead, GEP was lower in July compared to June and August in 2011 and 2012. A corresponding decline in RE was not observed.

Figure 8 shows cumulative NEP for the study period. All years experienced a negative trend in NEP until the start of the growing season, because RE is the only component flux during the dormant winter period. The earliest growing season start, shown by a positive trend in NEP, was in 2012. 2010 and 2006 also experienced a relatively early start to the growing season. Conversely, 2004 experienced the latest growing season start. Most years experienced a similar rate of increase in NEP between April and June. Exceptions to this were 2004 and 2012; these years experienced lower rates of NEP shown by lower slopes. After June, annual NEP diverged. In general, net uptake continued to increase until the end of the growing season in October. However, rates of increase remained relatively low in 2004, 2005 and 2012, resulting in the lowest observations of annual NEP. Overall, 2005 and 2012 showed nearly identical annual dynamics. Maximum and minimum annual NEP were observed in 2004 and 2011, respectively.

Annual values of GEP, RE, NEP and ET for the study period are shown in Table 3. Maximum and minumum annual GEP were observed in 2008 and 2005, respectively. Interannual variability was higher in annual RE than GEP. Maximum and minimum annual RE were observed in 2012 and 2011, respecitvely.

Table 3. Carbon and water dynamics throughout study period.

	2003	2004	2005	2006	2007	2008	2009	2010	2011	2012
GEP (g C m^{-2} year^{-1})	1427	1368	1264	1383	1309	1573	1411	1559	1427	1509
RE (g C m^{-2} year^{-1})	1185	1274	1090	1087	1054	1203	1011	1214	944	1350
NEP (g C m^{-2} year^{-1})	238	92	160	289	254	363	397	340	479	154
ET	401	411	424	491	449	529	484	539	486	501

Mean annual pre-thinning GEP was 1413 ± 102 g C m^{-2} year^{-1}; post-thinning GEP was 1509 g C m^{-2} year^{-1}. Mean annual pre- and post-thinning GEP were not significantly

different (p = 0.0225). Mean pre-thinning RE was 1118 ± 108 g C m^{-2} year^{-1}; post-thinning

RE was 1350 g C m^{-2} year^{-1}. Mean annual pre-thinning RE was significantly lower than post-

thinning (p < 0.01). Mean pre-thinning NEP was 290 ± 120 g C m^{-2} year^{-1}; post-thinning NEP

was 154 g C m^{-2} year^{-1}. Mean annual pre-thinning NEP was significantly greater than post-

thinning (p < 0.01).

Water dynamics were measured continuously throughout the study period. Annual

ET ranged from 401 mm to 539 mm (Table 3). Maximum and minimum annual ET were

observed in 2010 and 2003, respectively. Mean pre-thinning ET was 468 ± 50 mm; post-

thinning ET was 501 mm. Mean annual pre- and post-thinning ET were not significantly

different (p = 0.0825). Cumulative evapotranspiration (ET) is shown in Figure 9.

Cumulative ET was higher in 2012 than all other years until July. ET declined during July

and August, but returned to normal in September. Growing season ET was lowest in 2005.

Water use efficiency (WUE), the amount of productivity (GEP) per unit of water use

(ET) ranged from 2.8 to 3.6 g C kg^{-1} H$_2$O. Thinning did not affect WUE; mean pre-thinning

WUE was 3.0 ± 0.2 g C kg^{-1} H$_2$O and post-thinning WUE was 3.0 g C kg^{-1} H$_2$O.

3.3 Thinning effects on NEP, GEP and RE

Three different approaches were used to evaluate thinning effects on carbon

dynamics: (1) pre- and post-thinning carbon dynamics at TP39 were compared to two

nearby un-thinned forests (TP74 and TPD); (2) annual functional relationships between

NEP and key meteorological variables were evaluated; and (3) effects of variation in environmental drivers and biotic responses on carbon dynamics were assessed.

3.3.1 Comparison with nearby forest sites

Carbon dynamics in 2012 from an adjacent 39-year-old white pine plantation forest (TP74, Peichl et al. 2010a) and an 80-year-old deciduous forest (TPD, Parsaud 2013) located 20 km west of the thinned stand (TP39) were compared to TP39. TP74 and TPD were not thinned. We first compared the relationships between Ts and SM at TP39 and TP74 to evaluate whether gaps created in the canopy by the thinning operation affected these variables by increased light availability and air motion. Direct comparisons of the relationships indicated that Ts and SM were not affected by thinning (mean pre- and post-thinning R^2 for Ts were 0.98 and 0.99, respectively; mean pre- and post-thinning R^2 for SM were 0.80 and 0.87, respectively).

Figure 10 shows annual cumulative NEP for TP74, TP39 and TPD. TP74 fluxes were SI-normalized to account for differences in stand age. The start of the 2012 growing season began simultaneously at TP39 and TP74. The growing season started nearly two months later at TPD compared the coniferous sites because of the additional time required for deciduous leaf emergence. During the growing season, the highest rate of carbon uptake was observed at TPD, followed by TP74 and TP39. Both coniferous sites experienced a pronounced mid-summer decline in productivity in 2012, associated with hot and dry conditions; this was not observed to the same extent at TPD. The annual retention of most pine needles compared to the annual loss of all deciduous leaves via senescence resulted in

22

an earlier end to the growing season at TPD. At the coniferous sites, carbon dynamics diverged towards the end of the 2012 growing season. While NEP was maintained at approximately 400 g C m^{-2} between October and December at TP74, TP39 experienced a reduction in net productivity of approximately 50 g C m^{-2}. It is hypothesized that this reduction was driven by the decomposition of thinning-related residuals; these residuals may have required several months of warm temperatures and available water in order to begin breaking down and releasing CO_2, explaining the lagged effect.

Differences between annual SI-normalized carbon dynamics at TP39 and TP74 are shown in Figure 11. Between 2008-2012, normalized GEP, RE and NEP were higher on average at the younger site (by 45 g C m^{-2} year^{-1}, 44 g C m^{-2} year^{-1} and 1 g C m^{-2} year^{-1}, respectively). The greatest difference in annual NEP was observed in 2012, a combined effect of lower RE and higher GEP at TP74. RE was higher at TP39 for the majority of the 2012 growing season. Notably, normalized GEP was higher at TP74 than TP39 throughout all growing season months except July. This month was identified as extremely hot by the BHI, and was identified as having many water stress days. Higher GEP at TP39 during this extremely hot and dry month provides evidence for increased drought tolerance following thinning by reduced competition for water.

3.3.2 Functional relationships

The functional relationship between non-gapfilled NEP and binned Ta (bin size of 0.5°C) is shown in Figure 12. Peak NEP occurred at approximately 22°C for all years except 2003 and 2008. These years peaked at approximately 25°C. For any observed Ta, NEP was

lowest in 2005, 2007 and 2012. As previously described, 2005, 2007 and 2012 experienced

extremely hot and dry growing season conditions. Maximum Ta was observed in 2012.

Figure 13 shows the functional relationship between non-gapfilled NEP and binned

PAR (bin size of 50 µmol m^{-2} $second^{-1}$). Productivity plateaued at approximately 1500 µmol

m^{-2} $second^{-1}$ for all years except 2005, which showed a decline in NEP at higher rates of

radiation. Analogous to the functional relationship between NEP and Ta, 2005, 2007 and

2012 demonstrated the lowest rates of NEP for all levels of PAR.

The functional relationship between non-gapfilled NEP and binned VPD (bin size of

0.05 kPa) is shown in Figure 14. For most years, maximum productivity occurred between

0.7-1 kPa. At VPD values below 1 kPa, productivity was lowest in 2005, 2007 and 2012.

Highest values of VPD were also observed in these years, particularly 2012. Above 1 kPa,

the least productive year with increasing VPD was 2005. Conversely, 2012 became one of

the most productive years with increasing atmospheric demand for water vapor. This

provides further evidence for reduced competition for water and improved drought

tolerance following the removal of 30% of trees.

The relationship between non-gapfilled NEP and binned VWC (bin size of 0.05%) is

shown in Figure 15. Below VWC values of approximately 8% (i.e. 0.08 m^3 m^{-3}), productivity

is limited. Above VWC values of 8%, productivity becomes increasingly reduced. Therefore,

maximum productivity at this site occurs when VWC is approximately 8%. The relationship

between VWC and NEP is similar to that of Ta (Fig. 12) and PAR (Fig. 13) in that 2005, 2007

and 2012 generally demonstrated lowest rates of NEP compared to all other years. Below VWC values of 12%, lowest productivity was observed in 2004 and 2005; highest productivity was observed in 2011. Above 12% VWC, 2007 was least productive and 2008 and 2010 were most productive.

3.3.3 Crossed- meteorological and parameter year test

By crossing each 'meteorological year' with each 'parameter year', environmental driver and associated biotic response scenarios were generated for NEP (Fig. 16). Using 2012 model parameters and 2003-2012 meteorological data, NEP ranged between a minimum of 95 g C m^{-2} $year^{-1}$ (in 2006) and maximum of 338 g C m^{-2} $year^{-1}$ (in 2007) (Fig. 16a). Particularly low annual NEP from 2006 meteorological conditions and 2012 parameters was driven by elevated RE from high annual SM and Ts conditions. Using 2012 meteorological conditions and 2003-2012 model parameters resulted in higher variability; NEP ranged between 92 g C m^{-2} $year^{-1}$ (in 2004) and 625 g C m^{-} $year^{-1}$ (in 2011) (Fig. 16b). This emphasizes that variation in biotic responses to environmental forcing is responsible for more variation in NEP compared to meteorological conditions.

Predictions of GEP, RE and NEP from the crossed- meteorological and parameter year test (n = 100) were analyzed using ANOVA. Results were used to determine the magnitude of 'meteorological year' and 'parameter year' effects on annual fluxes, shown in Figure 17. Positive effects for RE indicate increased respiratory losses, whereas negative effects for GEP indicate reduced canopy uptake.

Relative to the average crossed-model prediction, 'parameter year' effects for GEP (Fig. 17a) ranged from -130 g C m^{-2} year^{-1} (in 2005) to +184 g C m^{-2} year^{-1} (in 2007). 'Meteorological year' effects were smaller, ranging from -103 g C m^{-2} year^{-1} (in 2003) to +94 g C m^{-2} year^{-1} (in 2010). At the annual time scale, GEP was more influenced by variability in model parameters (76%) than meteorological conditions (21%). Relative to the average crossed model prediction, 'parameter year' effects for RE (Fig. 17b) ranged from -198 g C m^{-2} year^{-1} (in 2011) to +162g C m^{-2} year^{-1} (in 2004). 'Meteorological year' effects were smaller, within ±90 g C m^{-2} year^{-1}. Annual RE was more influenced by variability in model parameters (81%) than meteorological conditions (19%). 'Parameter year' effects for NEP, relative to the average crossed model prediction, were also greater than meteorological year effects (Fig. 17c), ranging from -262 g C m^{-2} year^{-1} (in 2004) to +283 g C m^{-2} year^{-1} (in 2011), and -158 g C m^{-2} year^{-1} (in 2006) to +101 g C m^{-2} year^{-1} (in 2009), respectively. Similar to the other flux components, NEP was more influenced by variability in model parameters (76%) than meteorological conditions (23%). Overall, post-thinning 'parameter year' effects were not significantly different from pre-thinning effects, indicating that thinning did not significantly affect the biotic response to environmental drivers.

Results of multiple comparisons (not shown) give an indication of which years had more favorable meteorological conditions and model parameters for maximizing NEP. For 'meteorological year', the least favourable year was 2006. Years 2003 and 2012 were also less favourable compared to other years. Using 2003, 2006 and 2012 meteorological data with any year of model parameters resulted in relatively low NEP. The most favourable

'meteorological year' was 2009. For 'parameter year', the least favourable years were 2004 and 2012; 2011 was by far the most favourable. Modeling NEP with all years of meteorological data and 2004 and 2012 model parameters therefore resulted in relatively low annual NEP. In general, model results were consistent with observations. For example, 2004 was identified as the least favourable 'parameter year' for NEP; lowest NEP of all study years was observed in this year. The most favourable parameter year was identified as 2011; this year had the highest observed NEP, attributed to warm growing season Ta and abundant P (Fig. 2d). Finally, 2012 was one of the least favourable years for 'meteorological year' and 'parameter year', and it had one of the lowest observed annual NEP values.

CHAPTER 4: DISCUSSION

This study demonstrates the effects of climatic variability, extreme weather events and thinning on forest carbon dynamics in a 74-year-old white pine plantation in southern Ontario. We found that meteorological conditions were responsible for approximately 20% of interannual variability in carbon dynamics. Remaining variability was explained by factors including maximum GEP, the response of RE to Ta, and the size and distribution of the carbon pool (Richardson et al. 2007). Thinning did not significantly impact biotic responses to environmental conditions. Although NEP was reduced by an increase in RE in the first post-thinning year, the forest remained a net carbon sink. Further, results suggest that thinning may improve drought tolerance by improving access to water for remaining trees.

27

4.1 Climatic effects on GEP, RE and NEP

In general, extreme weather events, particularly heat and drought stress, affected annual carbon dynamics. Years that experienced heat and drought stress (i.e. 2004, 2005, 2007 and 2012) were generally associated with limited net carbon uptake, while moderate annual Ta and water availability resulted in higher net uptake (i.e. 2011).

Air and soil temperature, important factors in the growth and development of forest ecosystems, exhibited seasonal and interannual variability throughout the study period. NEP was positively correlated to growing season Ta until a peak threshold (approximately 23-25°C at TP39); rates of carbon uptake declined with increasing Ta above this threshold. Water availability was another important determinant of carbon dynamics at TP39. Consistent with Holst et al. (2008), we observed reduced NEP during periods of heat and drought stress (i.e. 2004, 2005, 2007 and 2012). Our results further support findings by Granier et al. (2007), who found that reductions in NEP associated with heat and drought stress were driven more by reductions in GEP than increases in RE in European coniferous forests.

Trends in early growing season Ta were also important factors for carbon uptake at TP39. For example, in 2004 cool spring Ta and abundant P resulted in a delayed start to the growing season compared to all other years, and contributed to low annual NEP (Fig. 8). Conversely, abnormally warm Ta during the start of the 2012 growing season caused increases in both GEP and RE; in previous years trees were still dormant during this time of year. Consistent with Barr et al. (2002), we found that during this unusually warm spring

28

period, soil respiration offset increases in carbon uptake. High Ta during spring months has also been shown to increase annual carbon sequestration in some forests (Goulden et al. 1996; Chen et al. 2009). Quantifying the effect of this on annual carbon dynamics was challenging for 2012 because of the difficulty in separating effects of thinning from effects of early spring Ta.

VPD exhibited variability at monthly and annual timescales. Previous work at this site determined that VPD was the primary control on forest water loss (MacKay et al. 2012). When the forest was not water-limited (VWC > 0.068 m^3m^{-3}), ET increased with VPD. Above this site-specific threshold, and when VPD was high (above 0.8-1 kPa), tree stomata closed to conserve water (Fig. 14) (McLaren et al. 2008; MacKay et al. 2012; Breshears et al. 2013). Limitation of photosynthesis associated with high Ta and VPD was observed at TP39 in 2005, 2007 and 2012. This was also observed in a ponderosa pine forest in California, USA (Goldstein et al. 2000).

Consistent with the findings of Richardson et al. (2007), the crossed- meteorological and parameter year test determined that at TP39, approximately 20% of the interannual variability in GEP and RE was explained by environmental conditions. Results for NEP were less consistent; we found that environmental conditions explain 20% of the interannual variability in NEP at TP39, compared to 40% observed by Richardson et al. (2007). Therefore, all components of annual fluxes (i.e. NEP, GEP and RE) were driven more by biotic responses to environmental drivers (i.e. maximum GEP, the response of RE to Ta and the size of the carbon pool) than by meteorological conditions. While meteorological

29

conditions, especially extreme weather events, are important to consider when evaluating

annual carbon dynamics, these results emphasize the significance of also considering

longer-term climatic conditions and factors such as disturbances. The forest management

practice of thinning was conducted at this site in 2012, and was predicted to affect biotic

responses to environmental drivers by altering functional responses of productivity and

the size and distribution of the carbon pool.

4.2 Thinning effects on GEP, RE and NEP

Overall, we found that in the first post-thinning year, effects of thinning on GEP, RE

and NEP were less substantial than expected based on reductions in LAI and BA (Saunders

et al. 2012; Scott et al. 2004). Consistent with the findings of Saunders et al. (2012), the

forest remained a net carbon sink, although NEP in the first post-thinning year was reduced

by increased RE. This differed from Dore et al. (2012), who found that a ponderosa pine

forest in Arizona, USA became a net carbon source in the first post-thinning year.

At TP39, model predicted RE with increasing Ts, and model predicted GEP with

increasing PAR, did not demonstrate significant effects of thinning (Fig. 5 and Fig. 6).

Further, post-thinning GEP and RE were within the ranges of interannual variability for the

study period. Increased understory growth, stimulated by increased light, water and

nutrient availability, likely compensated for thinning-related reductions in GEP (Vesala et

al. 2005; Campbell et al. 2009; Moreaux et al. 2011). Annual RE was slightly higher in 2012

compared to pre-thinning years. Annual RE was also higher at TP39 compared to the two

nearby forest sites, TP74 and TPD. This was unexpected for TPD because decomposition of

litterfall from the deciduous trees was predicted to drive higher annual RE. Plausible reasons for high post-thinning RE at TP39 include thinning-related increases in Ts and SM, soil disturbance and decomposition of thinning residues. A comparison between Ts and SM at both TP39 and TP74 refuted the former reason. Soil disturbance caused by the feller-buncher and forwarder may have been a contributing factor. Thinning operations are typically conducted when soil is frozen to minimize disturbance, however the mild winter Ta in 2012 did not allow for this. Nevertheless, effects of thinning on RE were less than expected considering the significant addition of thinning residues to the forest floor. Relatively slow decomposition rates of large thinning residues (i.e. large branches, crowns and roots) are the most probable explanation. It is expected that GEP and RE will increase over the next several years at this site as understory growth develops and thinning residues continue to decompose.

The crossed- meteorological and parameter year test determined that variation in the biotic response to environmental forcing (e.g., maximum GEP, response of RE to Ta, size and distribution of the carbon pool) accounted for approximately 80% of variation in annual GEP, RE and NEP. This finding is consistent with Richardson et al. (2007) for GEP and RE. Functional relationships between productivity (i.e. unfilled NEP) and key meteorological variables (i.e. Ta, PAR, VPD and VWC) in 2012 were within the range of interannual variability. For Ta, PAR and VWC, the least productive years for given meteorological conditions were 2005, 2007 and 2012. This was attributed to inadequate growing season conditions (i.e. heat and drought stress) rather than physiological changes caused by disturbances. Similar to findings by Dore et al. (2012), we did not observe an

impact of thinning on WUE. Thinning also changed the size and distribution of the carbon pool by the removal of boles from the stand and the addition of crowns, branches and foliage to the forest floor. Most importantly, despite changes to the carbon pool, thinning did not significantly impact biotic responses to environmental conditions. Two non-thinning years (i.e. 2004 and 2011) exhibited greater 'parameter year' effects than 2012.

Our results support previous studies that have reported increased drought tolerance following thinning (Dore et al. 2010; Dore et al. 2012). Differences in carbon uptake between TP39 and TP74 provide evidence of improved drought tolerance. While both sites experienced a decline in carbon uptake associated with extremely hot and dry conditions in July 2012, the extent of the decline was greater at TP74. This suggests that thinning may have reduced the limitation of drought on carbon uptake during the summer, as was observed in a ponderosa pine stand following thinning (Dore et al. 2010). The functional relationship between VPD and productivity (NEP) at TP39 provides further evidence of improved drought tolerance following thinning. When VPD was above 0.8 kPa, 2012 was more productive than pre-thinning years despite the increasing atmospheric demand for water vapour. This was attributed to improved drought tolerance by reduced competition for water following thinning. In contrast to Dore et al. (2012), the functional relationship between Ta and productivity was not affected by thinning at this site.

4.3 Implications and directions for future research

Forests represent a significant carbon sink in the global carbon cycle, and maximizing the amount of carbon sequestered by these ecosystems is an important climate

change mitigation strategy (Beer et al. 2010). Improving adaptation of forests to climate change, especially to heat and drought stress, is another important challenge facing forest managers, as these conditions are expected to become more frequent and severe in the future (Field et al. 2012). Results of this study may be used to modify current management practices in temperate coniferous forests to increase carbon sequestration and improve tolerance to environmental stress. In the past, the shelterwood silviculutral system has been a common practice in managed pine plantations, used to reduce resource competition, stimulate growth for timber production and enhance long-term carbon sequestration. Results of this study indicate that in temperate coniferous forests, this management practice may also be an effective tool in the improvement of drought stress tolerance (Dore et al. 2010; Dore et al. 2012).

The extent to which climatic conditions in a given year influence forest growth conditions in future years (lagged effects) may be a source of uncertainty in this study (Braswell et al. 1997). Continuation of flux measurements at this site will further improve the understanding of thinning effects on carbon dynamics in temperate coniferous forests, because some processes (e.g. decomposition of thinning residues) operate on time scales longer than one year. Evaluating methods by which lagged climate effects may be estimated and controlled for would also benefit this area of study. Further research at this site is also needed to quantify the extent to which understory growth compensated for thinning-related reductions in productivity (Campbell et al. 2009). Soil respiration measurements may also be evaluated to better understand effects of thinning residues on ecosystem-level respiration.

CHAPTER 5: CONCLUSIONS

Our study found that in the first post-thinning year, effects of thinning on carbon dynamics in a temperate coniferous forest were less substantial than expected based on reductions in leaf area index and basal area. Although the forest remained a net carbon sink in the first year following the operation, post-thinning NEP was less than the pre-thinning mean (2003-2011). The reduction in NEP associated with the removal of 30% of trees from the stand was very similar to the effects of extreme heat and drought stress. This was shown by similarities in NEP between a year that experienced heat and drought stress (2005) and the post-thinning year (2012). Thinning-related reductions in NEP were driven by increased RE; GEP was not significantly affected. Increased understory growth, stimulated by increased availability of light, water and nutrients, likely compensated for reductions in GEP caused by the reduced photosynthetic capacity of the forest. Results also indicate that thinning may improve drought stress tolerance in temperate coniferous forests by improving water availability for remaining trees.

In general, although climatic variables were shown to explain less interannual variability in carbon dynamics compared to biotic responses to environmental drivers, extreme weather events, particularly heat and drought stress, affected annual carbon uptake. Years that experienced heat and drought stress (i.e. 2004, 2005, 2007 and 2012) were generally associated with low net carbon uptake, while a year with moderate temperatures and water availability (i.e. 2011) demonstrated high net carbon uptake.

Overall, our study highlights the potential to maximize long-term carbon sequestration and improve drought stress tolerance in temperate coniferous forest ecosystems through effective management practices.

REFERENCES

Arain, M. and Restrepo-Coupe, N. (2005). Net ecosystem production in a temperate pine plantation in southeastern Canada. Agricultural and Forest Meteorology. 128: 223-241.

Aubinet, M., Grelle, A., Ibrom, A., Rannik, U., Noncrieff, J., Foken, T. et al. (2000). Estimates of the annual net carbon and water exchange of forests: The EUROFLUX methodology. Advances in Ecological Research. 30: 113-175

Aubinet, M., Vesala, T. and Papale, D. (2012). *Eddy Covariance: A Practical Guide to Measurement and Data Analysis*. New York: Springer, 2012. 174-204. Print.

Baldocchi, D. (2003). Assessing the eddy covariance technique for evaluating carbon dioxide exchange rates of ecosystems: past, present and future. Global Change Biology. 9:479–492

Baldocchi, D., Falge, E., Gu, L., Olson, R., Hollinger, D., Running, S. et al. (2001). Fluxet: A new tool to study the temporal and spatial variability of ecosystem-scale carbon dioxide, water vapor, and energy flux densities. Bulletin of the American Meteorological Society. 82: 2415-2434.

Baldocchi, D. (2008). 'Breathing' of the terrestrial biosphere: Lessons learned from a global network of carbon dioxide flux measurement systems. Australian Journal of Botany. 56:1-26.

Barr, A.G., Griffis. T.J., Black, T.A., Lee, X., Staebler, R.M., Fuentes, J.D., Chen, Z. and Morgenstern, K. (2002). Comparing the carbon balances of boreal and temperate deciduous forest stands. Canadian Journal of Forest Research. 32: 813–822.

Barr, A., Richardson, A., Hollinger, D., Papale, D., Arain, M.A., Black, T., Bohrer, G., Dragoni, D. et al. (2012). Use of change-point detection for friction-velocity threshold evaluation in eddy covariance studies. Agricultural and Forest Meteorology. 171: 31-45.

Beaumont, L., Pittman, A., Perkins, S., Zimmermann, N., Yoccoz, N. and Thuiller, W. (2011). Impacts of climate change on the world's most exceptional ecoregions. Proceedings of the National Academy of Sciences. 108(6): 2306-2311.

Beer, C., Reichstein, M., Tomelleri, E., Ciais, P., Jung, M., Carvalhais, N. et al. (2010). Terrestrial gross carbon dioxide uptake: Global distribution and covariation with climate. Science. 329(5993): 834-838.

Bettinger, P., Boston, K., Siry, J. and Grebner, D. (2009). Forest management and planning. Burlington, MA: Academic Press

Bonan, G. (2008). Ecological climatology (2nd ed.). Cambridge: Cambridge University Press.

Braswell, B., Schimel, D., Linder, E. and Moore, B. (1997). The response of global terrestrial ecosystems to interannual temperature variability. Science. 278: 870-872.

Breshears, D., Adams, H., Eamus, D., McDowell, N., Law, D., Will, R. et al. (2013). The critical amplifying role of increasing atmospheric moisture demand on tree mortality and associated regional die-off. Frontiers in Plant Science. 4:1-4.

Brodeur, J.J. (2013). Data methods and analyses for sustainable operation and defensible results of a long-term, multi-site ecosystem flux measurement program. McMaster University, School of Geography and Earth Sciences, Doctor of Philosophy Dissertation.

Campbell, J., Alberti, G., Martin, J. and Law, B. (2009). Carbon dynamics of a ponderosa pine plantation following thinning treatment in the northern Sierra Nevada. Forest Ecology and Management. 257:453-463.

Chen, W.J., Black, T.A., Yang, P.C., Barr, A.G., Neumann, H.H., Nesic, Z. et al. (2009). Effects of climate variability on the annual carbon sequestration by a boreal aspen forest. Global Change Biology. 5:41-53.

Chen, J.M., Govind, A., Sonnentag, O., Zhang, Y., Barr, A. and Amiro, B. (2006). Leaf area index measurements at Fluxnet Canada forest sites. Agricultural and Forest Meteorolology. 140: 257–268.

D'Amato, A., Bradford, J., Fraver, S. and Palik, B. (2011). Forest management for mitigation and adaptation to climate change: Insights from long-term silviculture experiments. Forest Ecology and Management. 262: 803-816.

Dixon, R.K., Brown, S., Houghton, R. A., Solomon, M., Trexler, C. and Wisniewski, J. (1994). Carbon pools and flux of global forest ecosystems. Science. 263:185-189.

Dore, S., Kolb, T.E., Montes-Helu, M., Eckert, S.E., Sullivan, B.W., Hungate, B.A., Kaye, J.P., Hart, S.C., Kock, G.W. and Finkral, A. (2010). Carbon and water fluxes from ponderosa pine forests disturbed by wildfire and thinning. Ecological Applications. 20(3):663-683.

Dore, S., Montes-Helu, M., Hart, S.C., Hungate, B.A., Koch, G.W., Moon, J.B., Finkral, A.J. and Kolb, T.E. (2012). Recovery of ponderosa pine ecosystem carbon and water fluxes from thinning and stand-replacing fire. Global Change Biology. 18(10): 3171-3185.

Elliott, K., Stinson, A., Williams, S., Cleland, E. and Morneault, A. (2011). Tree marking prescription. Ontario Ministry of Natural Resources.

Environment Canada (2013). 1981-2010 Climate Normals and Averages. Retrieved 28 August, 2013 from: http://climate.weather.gc.ca/climate_normals/.

Field, C., Barros, V., Stocker, T., Dahe, Q., Jon Dokken, D., Ebi, K. et al. (2012). Managing the Risks of Extreme Events and Disasters to Advance Climate Change Adaptation. New York, NY: Intergovernmental Panel on Climate Change, Cambridge University Press.

Fluxnet (2013). Historical Site Status. Retrieved 26 September, 2013 from http://fluxnet.ornl.gov/site_status.

Goldstein, A., Hultman, N., Fracheboud, J., Bauer, R., Panek, J., Xu, M., Qi, Y., Guenther, A. et al. (2000). Effects of climate variability on the carbon dioxide, water, and sensible heat fluxes above a ponderosa pine plantation in the Sierra Nevada (CA). Agricultural and Forest Meteorology. 101:113-129.

Gower, S.T., Krankina, O.N., Olson, R.J., Apps, M.J., Linder, S. and Wang, C. (2001). Net primary production and carbon allocation patterns of boreal forest ecosystems. Ecological Applications. 11(5): 1395-1411.

Granier, A., Reichstein, M., Breda, N., Janssens, I.A., Falge, E. et al. (2007). Evidence for soil water control on carbon and water dynamics in European forests during the extremely dry year: 2003. Agricultural and Forest Meteorology. 143: 123–145.

Hansen, A., Neilson, R., Dale, V., Flather, C., Iverson, L., Currie, D., Shafer, S., Cook, R. and Bartlein, P. (2001). Global change in forests: responses of   species, communities, and biomes. Bioscience. 51: 765-779.

Holst, J., Barnard, R., Brandes, E., Buchmann, N., Gessler, A. and Jaeger L. (2008). Impacts of summer water limitation on the carbon balance of a Scots pine forest in the southern upper Rhine plain, Agricultural and Forest Meteorology. 148: 1815-1826.

Kljun, N., Rotach, M.W. and Schmid, H.P. (2002). A 3-D backward Lagrangian footprint model for a wide range of boundary layer stratifications. Bound Layer Meteorology. 103: 205–226.

Kljun, N., Calanca, P., Rotach, M.W. & Schmid H.P. (2004). A simple parameterisation for flux footprint predictions. Bound Layer Meteorology. 112: 503–523.

Kula, M. (2013). McMaster University, School of Geography and Earth Sciences, Master of Science Thesis. (unpublished).

Ledig, F. and Kitzmiller, J. (1992). Genetic strategies for reforestation in the face of global climate change. Forest Ecology and Management. 50: 153-169.

MacKay, S., Arain, M.A., Khomik, M., Brodeur, J., Schumacher, J., Hartmann, H. et al. (2012). The impact of induced drought on transpiration and growth in a temperate pine plantation forest. Hydrological Processes. 26(12): 1779-1791.

McLaren, J., Arain, M.A., Khomik, M., Peichl, M. and Brodeur, J. (2008). Water flux components and soil water-atmospheric controls in a temperate pine forest growing in a well-drained sandy soil. Journal of Geophysical Research. 113: 1-16.

Moreaux, V., Lamaud, E., Bosc, A., Bonneford, J.M, Medlyn, B. and Loustau, D. (2011). Paired comparison of water, energy and carbon exchanges over two young maritime pine stands (Pinus pinaster Ait.): effects of thinning and weeding in the early stage of tree growth. Tree Physiology. 31:903-921.

Pan, Y., Birdsey, R., Fang, J., Houghton, R., Kauppi, P., Kurz, W. et al. (2011). A large and persistent carbon sink in the world's forests. Science. 333: 988-992.

Papale, D., Reichestin, M., Aubinet, M., Canfora, E., Bernhofer, C., Kutsch, W. et al. (2006). Towards a standardized processing of Net Ecosystem Exchange measured with eddy covariance technique: algorithms and uncertainty estimation. Biogeosciences. 3:571-583.

Parsaud, A. (2013). Carbon exchange in a temperate deciduous forest. McMaster University, School of Geography and Earth Sciences, Master of Science Thesis.

Parresol, B. and Vissage, J. (1998). White pine site index for the Southern Forest Survey. U.S. Department of Agriculture, Forest Service, Southern Research Station, Ashville, N.C., 8pp.

Peichl, M. and Arain, M.A. (2006). Above- and belowground ecosystem biomass and carbon pools in an age-sequence of temperate pine plantation forests. Agricultural and Forest Meteorology. 140: 51-63.

Peichl, M. and Arain, M.A. (2007). Allometry and partitioning of above- and belowground tree biomass in an age-sequence of white pine forests. Forest Ecology and Management. 253:68-80.

Peichl, M., Arain, M.A. and Brodeur, J. (2010a). Age effects on carbon fluxes in temperate pine forests. Agricultural and Forest Meteorology. 150: 1090-1101.

Peichl, M., Brodeur, Khomik, M. and Arain, M. (2010b). Biometric and eddy covariance based estimates of carbon fluxes in an age-sequence of temperate pine forests. Agricultural and Forest Meteorology. 150: 952-965.

Presant, E.W. and Acton, C.J. (1984). The Soils of the Regional Municipality of Haldimand-Norfolk. Volume 1. Report No. 57. Agriculture Canada, Ministry of Agriculture and Food, Guelph, Ontario, 100 pp.

Raffaelli, D. and Frid, C. (Eds.). (2010). Ecosystem ecology: A new synthesis (1st ed.). Cambridge: Cambridge University Press.

Restrepo-Coupe, N. and Arain, M.A. (2005). Energy and water exchanges from a temperate pine plantation forest. Hydrological Processes. 19:27-49.

Reichstein, M., Falge, E., Baldocchi, D., Papale, D., Valentini, R., Aubinet, M., et al. (2005). On the separation of net ecosystem exchange into assimilation and ecosystem respiration: review and improved algorithm. Global Change. 11(9): 1424-1439.

Richardson, A.D., Hollinger, D.Y., Aber, J.D., Ollinger, S.V. and Braswell, B.H. (2007). Environmental variation is directly responsible for short- but not long-term variation in forest-atmosphere carbon exchange. Global Change Biology. 13:788-803.

Saunders, M., Tobin, B., Black, K., Gioria, M., Nieuwenhuis, M. and Osborne, B. (2012). Thinning effects on the net ecosystem carbon exchange of a Sitka spruce forest are temperature-dependent. Agricultural and Forest Meteorology. 157: 1-10.

Scott, N., Rodrigues, C., Hughes, H., Lee, J., Davidson, E., Dail, D. and Malerba, P. (2004). Changes in carbon storage and net carbon exchange after one year after an initial shelterwood harvest at Howland Forest, ME. Environmental Management. 33: 9-22.

Ontario Ministry of Natural Resources. (2011a). Annual Report on Forest Management. Queen's Printer for Ontario. 105pp. Retrieved 10 September 2013 from http://www.mnr.gov.on.ca/stdprodconsume/groups/lr/@mnr/@forests/documents/document/stdprod_101892.pdf

Ontario Ministry of Natural Resources. (2011b). Silvicultural systems. Retrieved 3 April 2013 from http://www.mnr.gov.on.ca/en/Business/Forests/2ColumnSubPage/STEL02_166048.html

Smith, D., Larson, B., Kelty, M. and Ashton, P.M. (1997). The practice of silviculture: Applied forest ecology (9th ed.). New York: John Wiley & Sons, Inc.

Spittlehouse, D., and Stewart, R. (2003). Adaptation to climate change in forest management. BC Journal of Ecosystems and Management. 4(1): 1-11.

Vesala, T., Suni, T., Rannik, U., Keronen, P., Markkanen, T., Sevanto, S. et al. (2005). Effect of thinning on surface fluxes in a boreal forest. Global Biogeochemical Cycles. 19(2): 1-11.
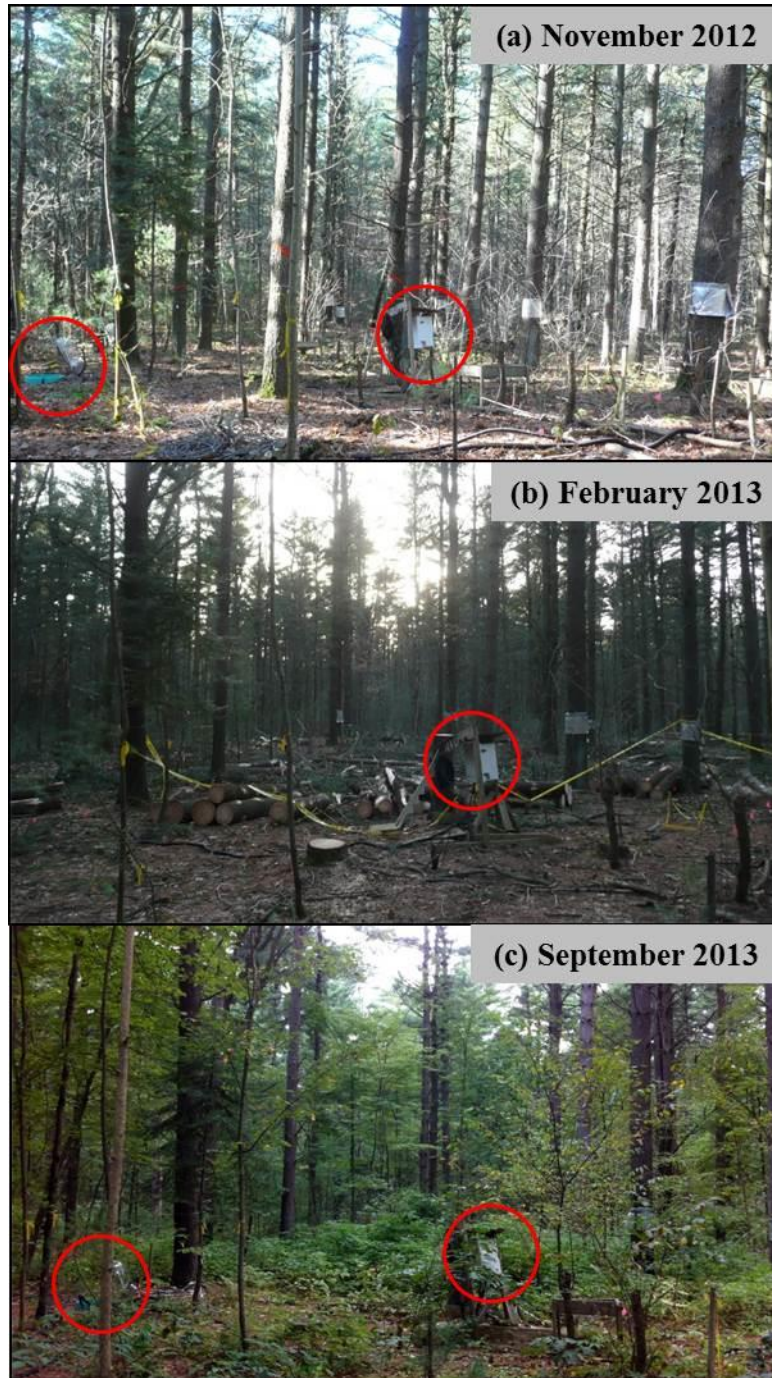
FIGURES

Figure 1. Photographs of an area of the stand near the flux tower (a) before thinning, (b) immediately after thinning and (c) 18 months after thinning. Growth of understory vegetation is evident in (c). Red circles identify the data logger and soil respiration chamber visible in each photo. Soil chambers were removed during the thinning operation.
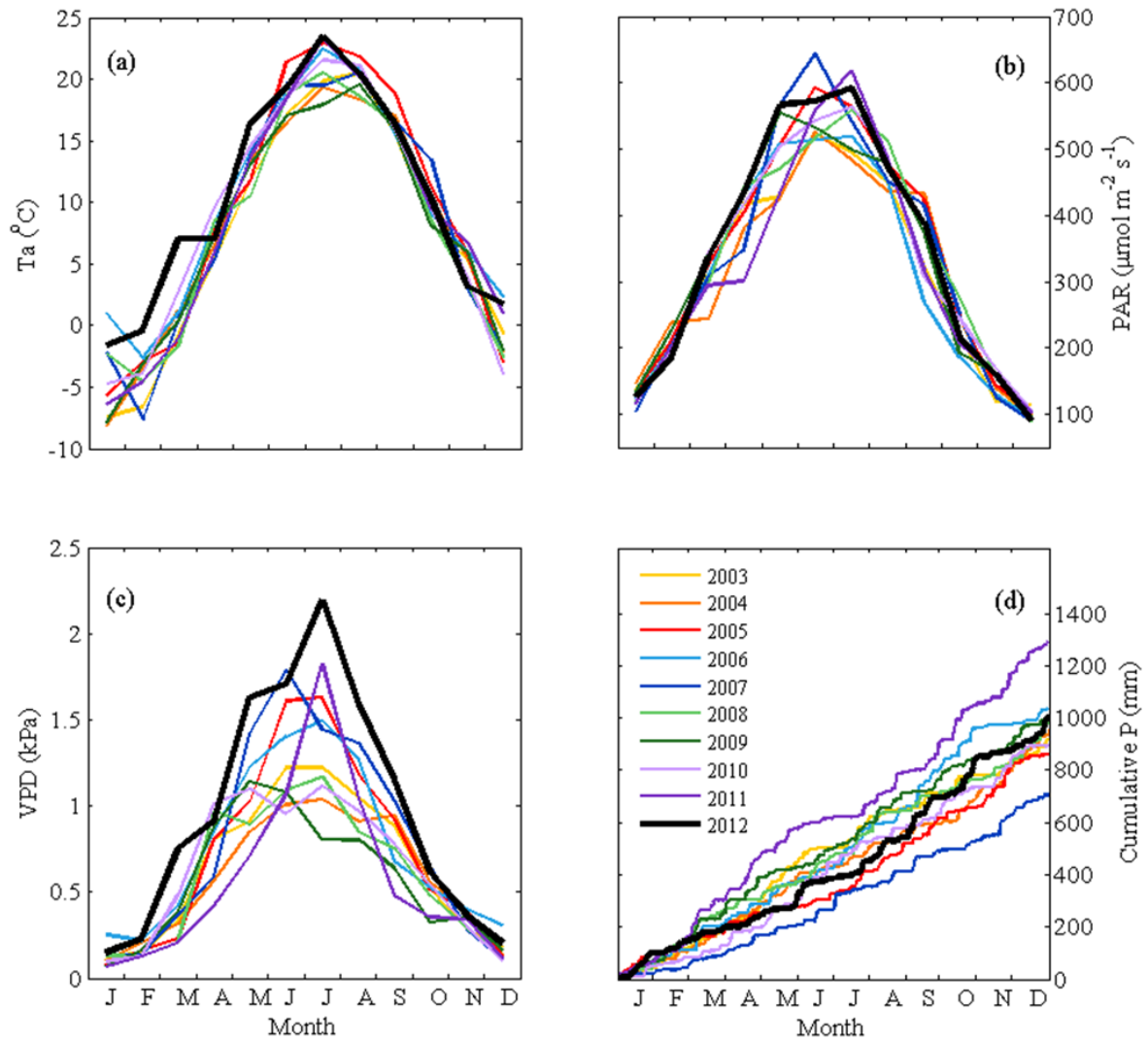
Figure 2. Monthly average air temperature (Figure 1a, Ta, °C), monthly average photosynetically active radiation (Figure 1b, PAR, µmol m^{-2} s^{-1}) , monthly maximum vapor pressure deficit (Figure 1c, VPD, kPa) and cumulative precipitation (Figure 1d, P, mm) throughout the study period.
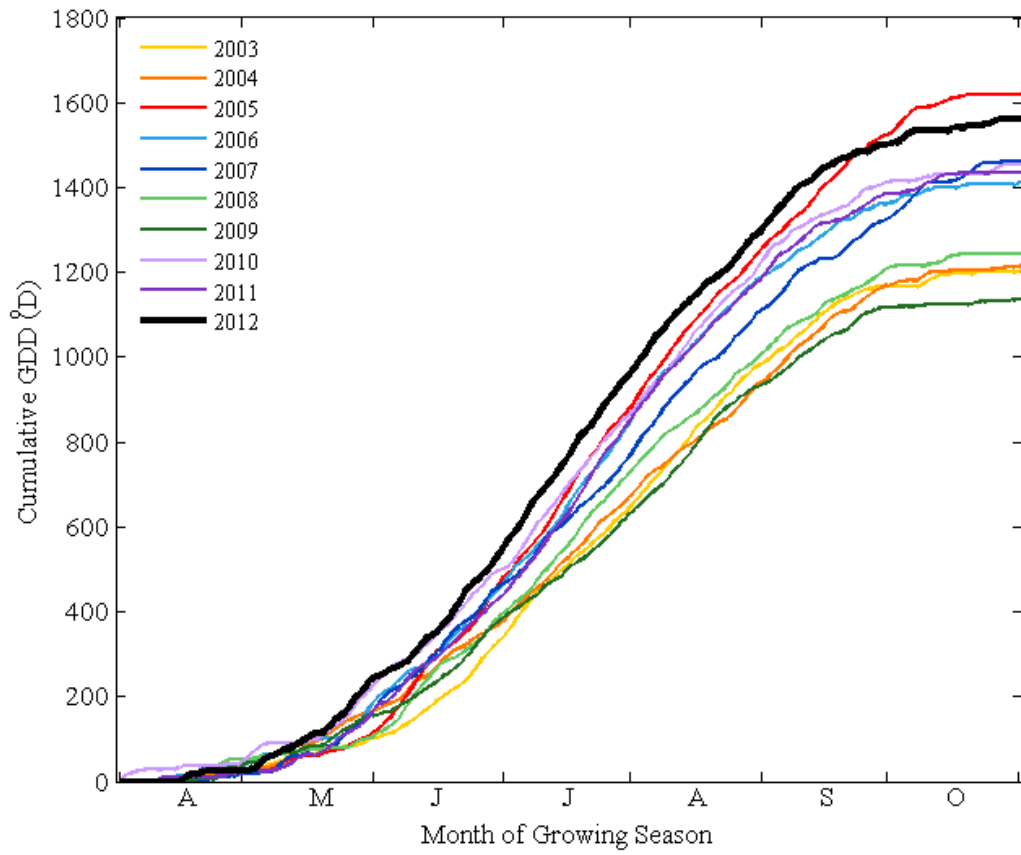
Figure 3. Cumulative growing degree days (GDD, °D) for the study period growing seasons (April 1 – October 31).
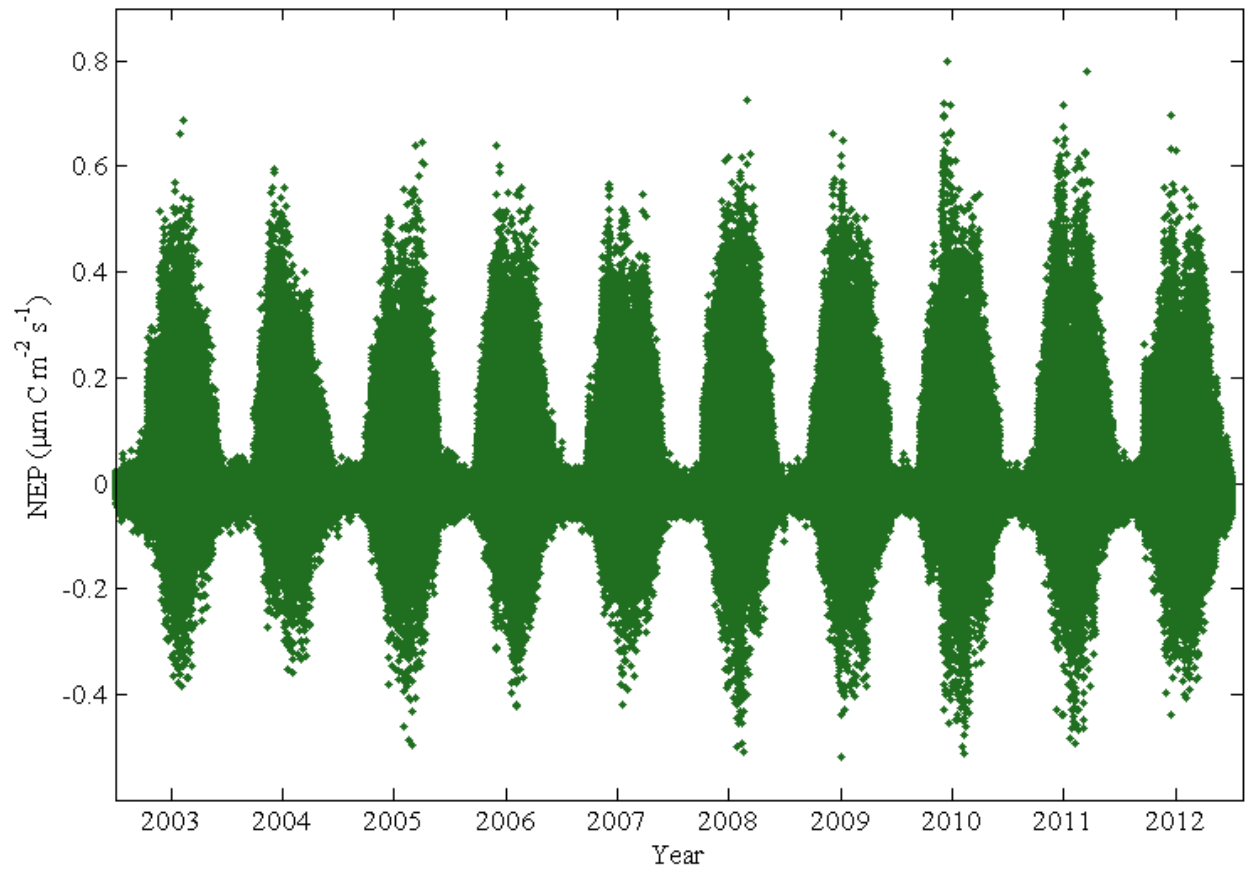
Figure 4. Half-hourly non-gapfilled net ecosystem productivity (NEP, μm C m^{-2} second^{-1}) for the study period.
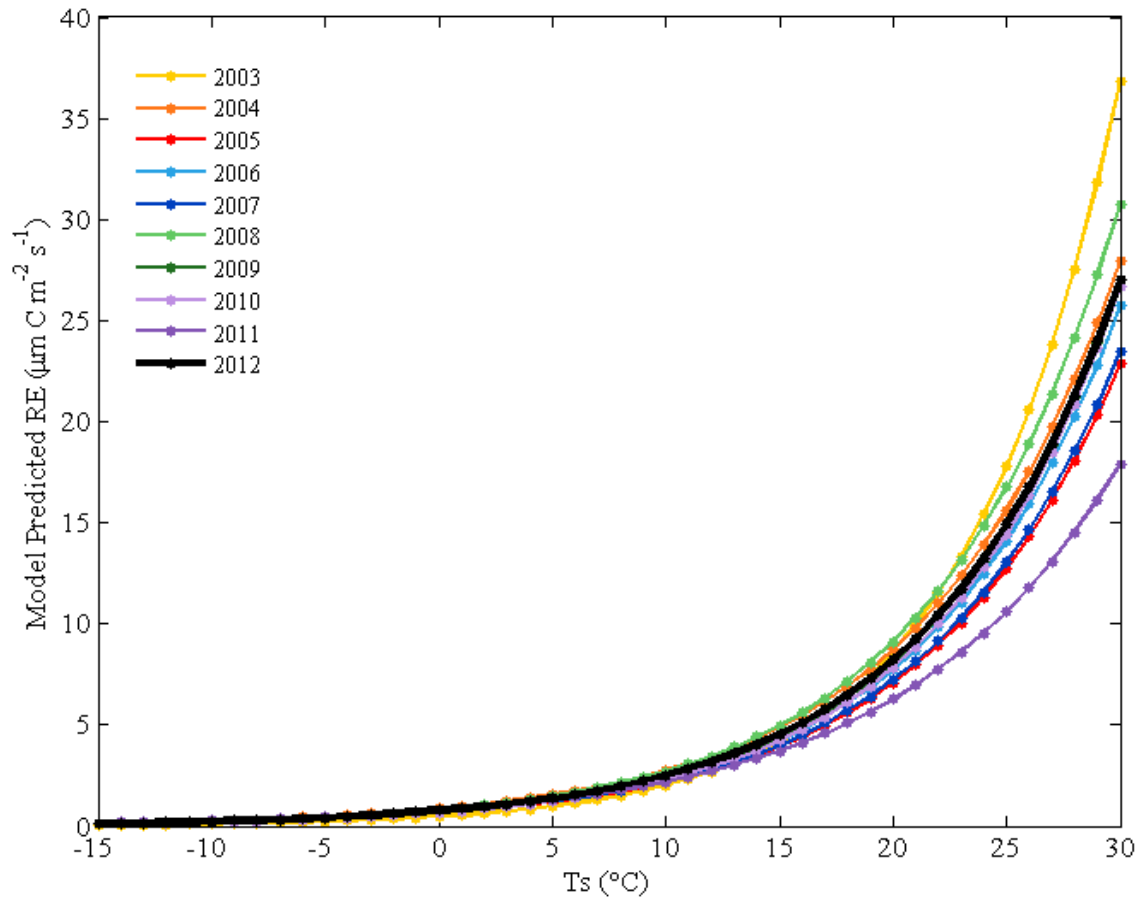
Figure 5. Model predicted ecosystem respiration (RE, μm C m^{-2} second^{-1}) with increasing soil temperature (Ts, °C).

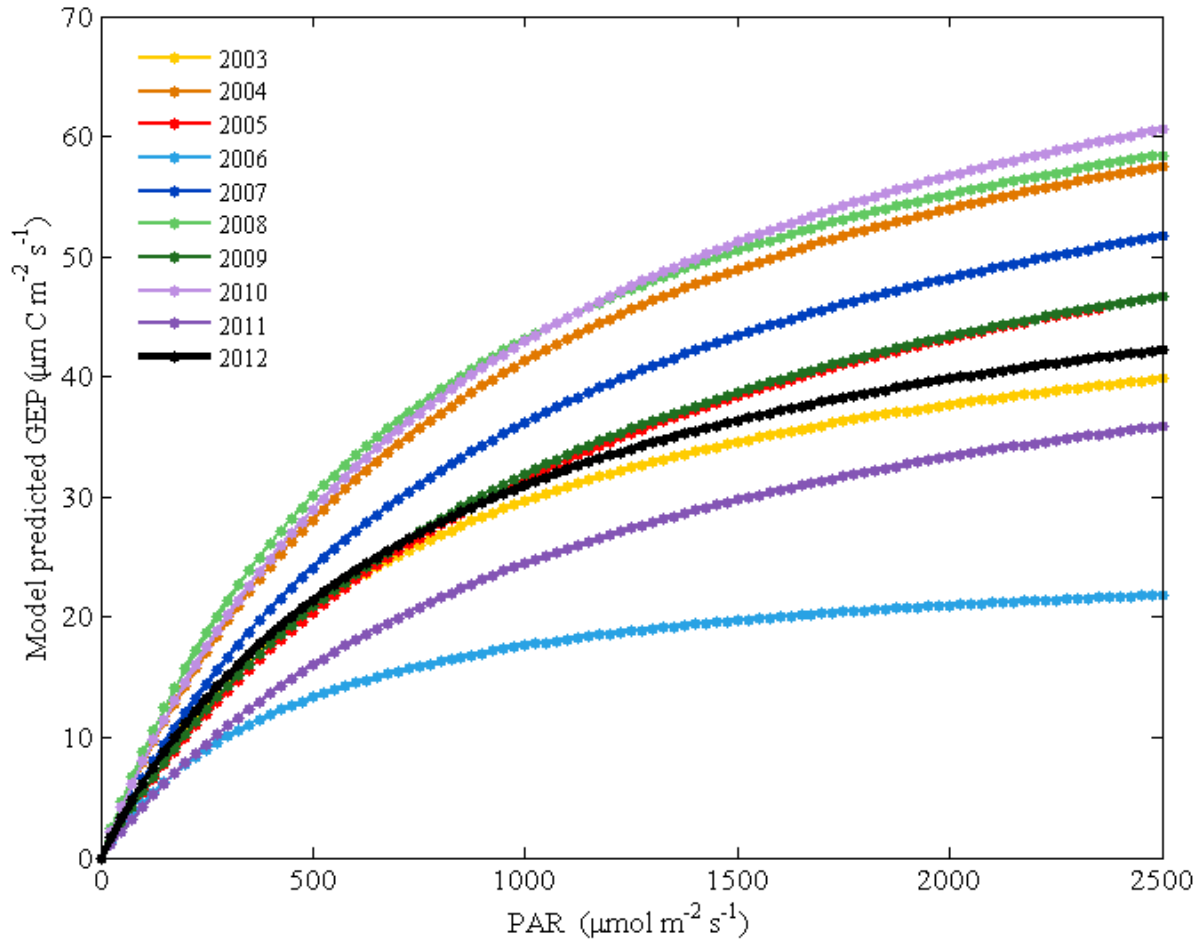**Figure 6**. Model predicted gross ecosystem productivity (GEP, μm C m^{-2} second^{-1}) with increasing photosynthetically active radiation (PAR, μmol m^{-2} second^{-1}).
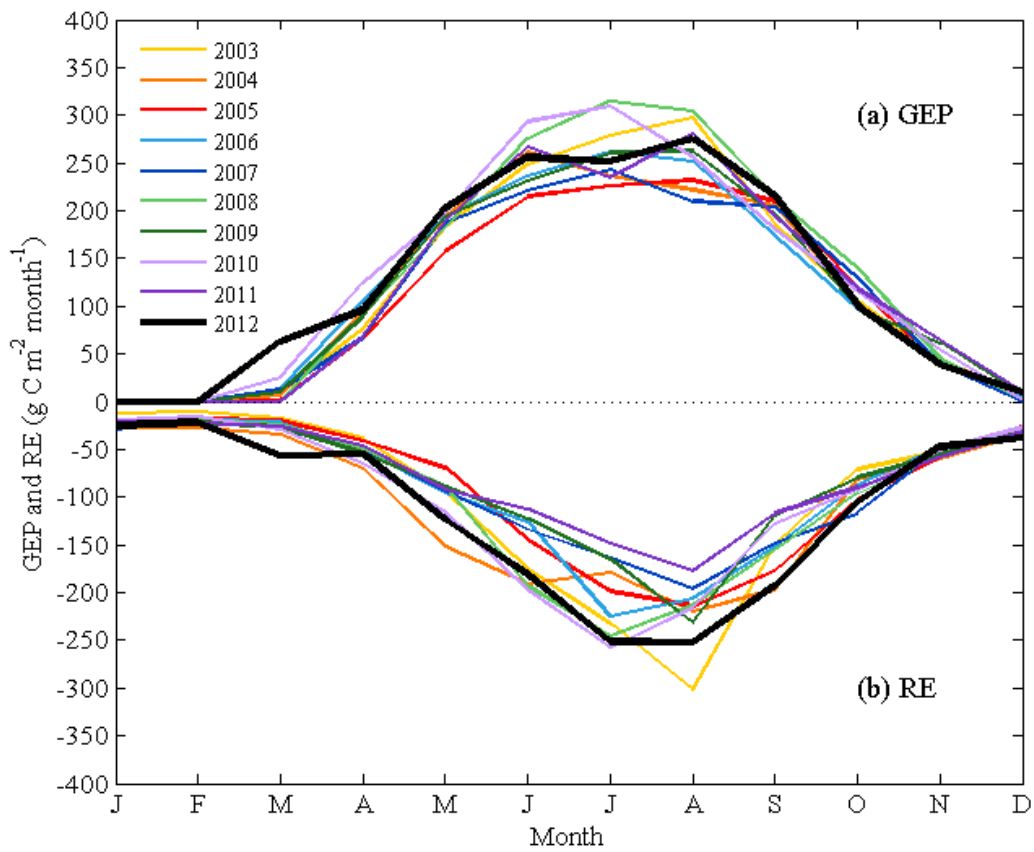
Figure 7. Monthly average gross ecosystem productivity (GEP, g C m^{-2} month^{-1}) and ecosystem respiration (RE, g C m^{-2} month^{-1}) for the study period.
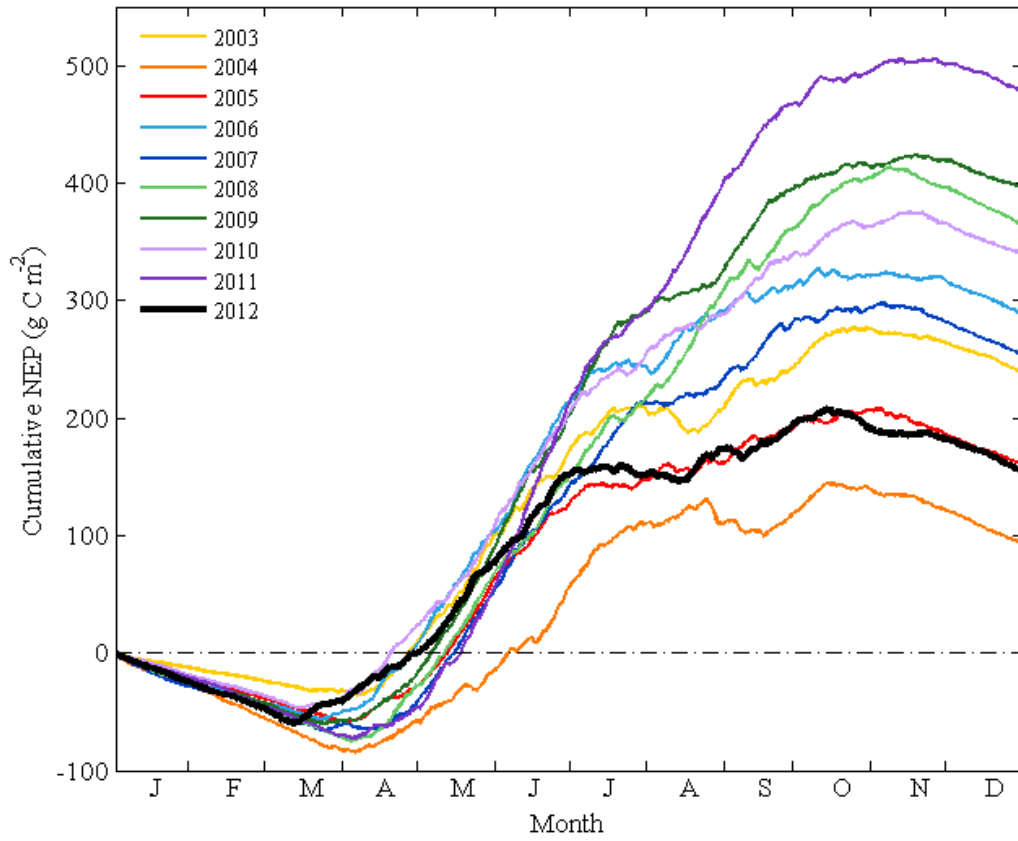
Figure 8. Cumulative net ecosystem productivity (NEP, g C m^{-2}) for the study period.
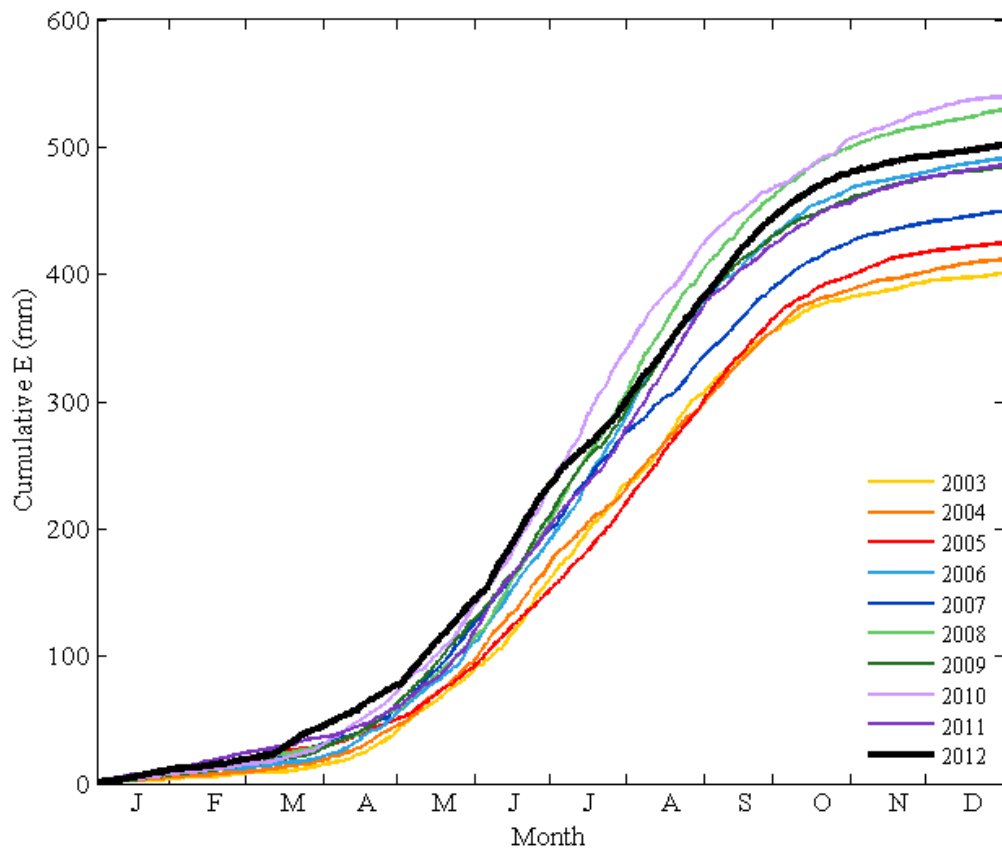
Figure 9. Cumulative evapotranspiration (ET, mm) for the study period.
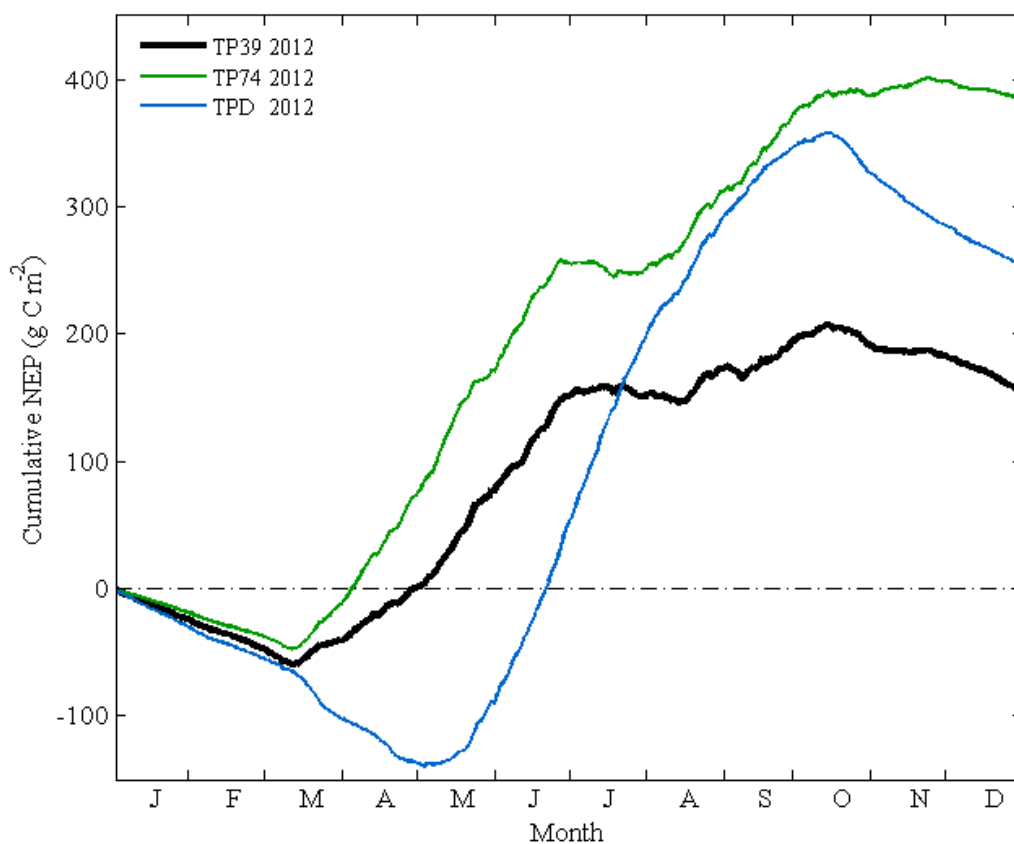
Figure 10. Cumulative net ecosystem productivity (NEP, g C m^{-2}) in 2012 for the thinned 74-year-old stand (TP39), a nearby 39-year-old white pine stand (TP74) and a nearby 80-year-old deciduous stand (TPD). TP74 fluxes were site index (SI) -normalized to account for differences in stand age.
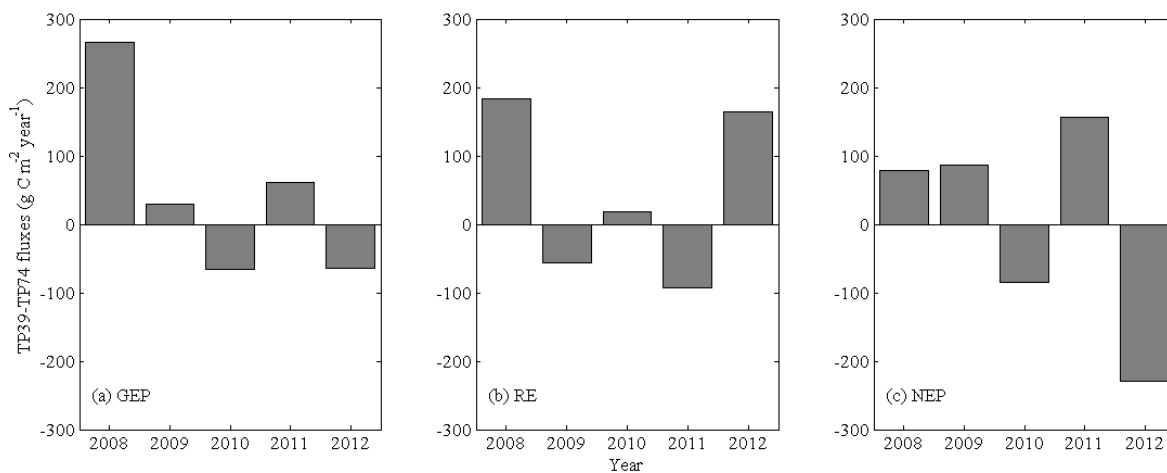
Figure 11. Differences in annual carbon fluxes (g C m^{-2} year^{-1}) between the 74-year-old stand (TP39) which was thinned in 2012, and a nearby unthinned 39-year-old stand (TP74). Fluxes at TP74 were site index (SI) -normalized to account for differences in stand age. Positive values indicate that fluxes were higher at TP39; negative values indicate that fluxes were higher at TP74.
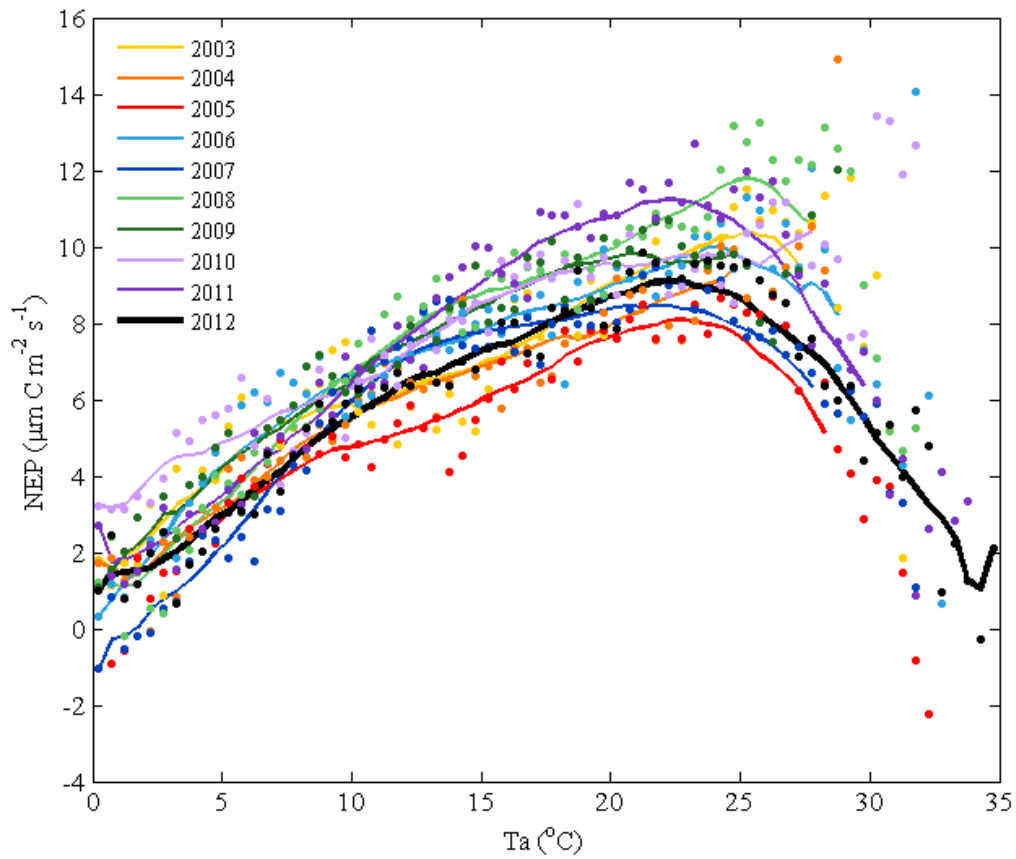
Figure 12. Relationship between daytime growing season measurements of binned air temperature (Ta, bin size of 0.5 °C) and non-gapfilled net ecosystem productivity (NEP, μm C m^{-2} second^{-1}). Solid lines show the moving average for each year. The stand was thinned in winter 2012.
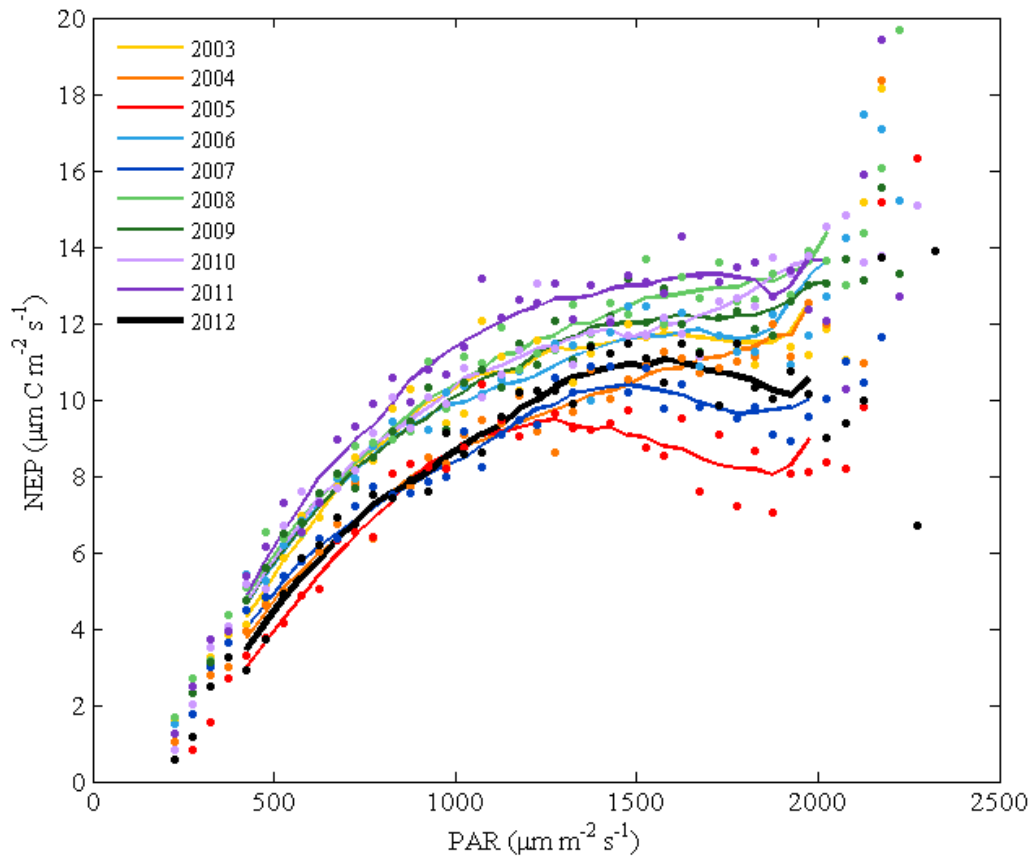
Figure 13. Relationship between daytime growing season measurements of binned photosynthetically active radiation (PAR, bin size of 50 μmol m^{-2} second^{-1}) and non-gapfilled net ecosystem productivity (NEP, μm C m^{-2} second^{-1}). Solid lines show the moving average for each year. The stand was thinned in winter 2012.
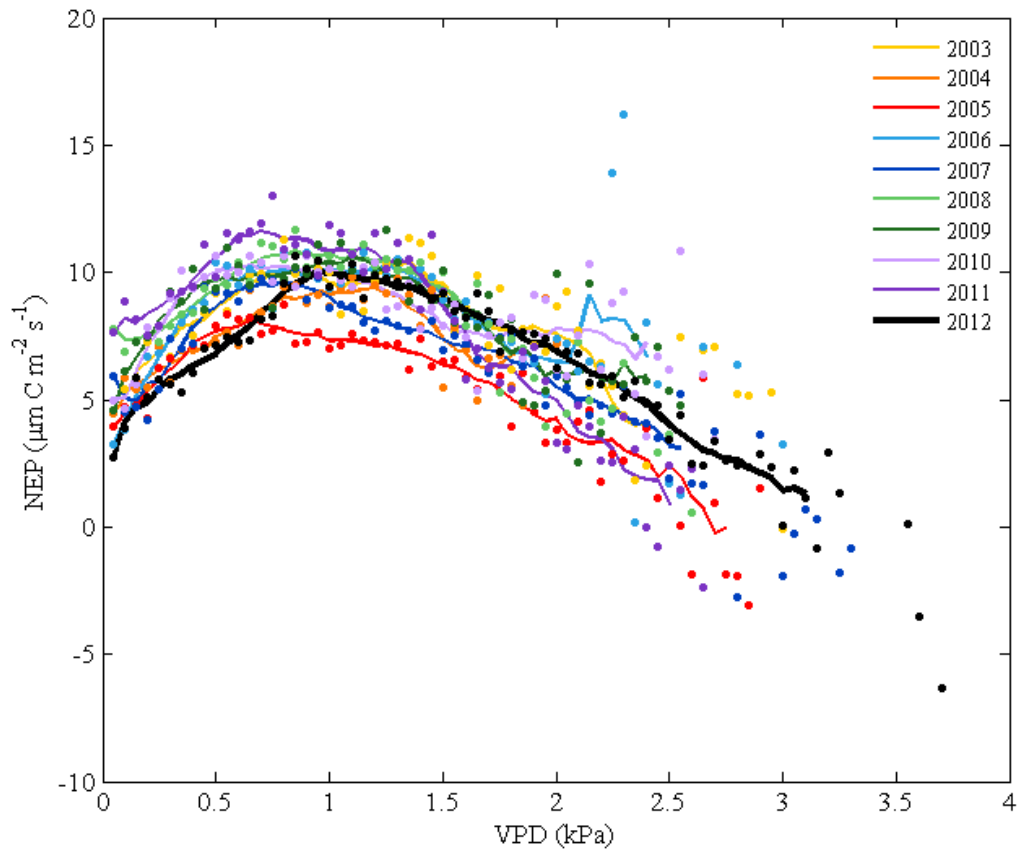
Figure 14. Relationship between daytime growing season measurements of binned vapor pressure deficit (VPD, bin size of 0.05 kPa) and non-gapfilled net ecosystem productivity (NEP, μm C m^{-2} second^{-1}). Solid lines show the moving average for each year. The stand was thinned in winter 2012.
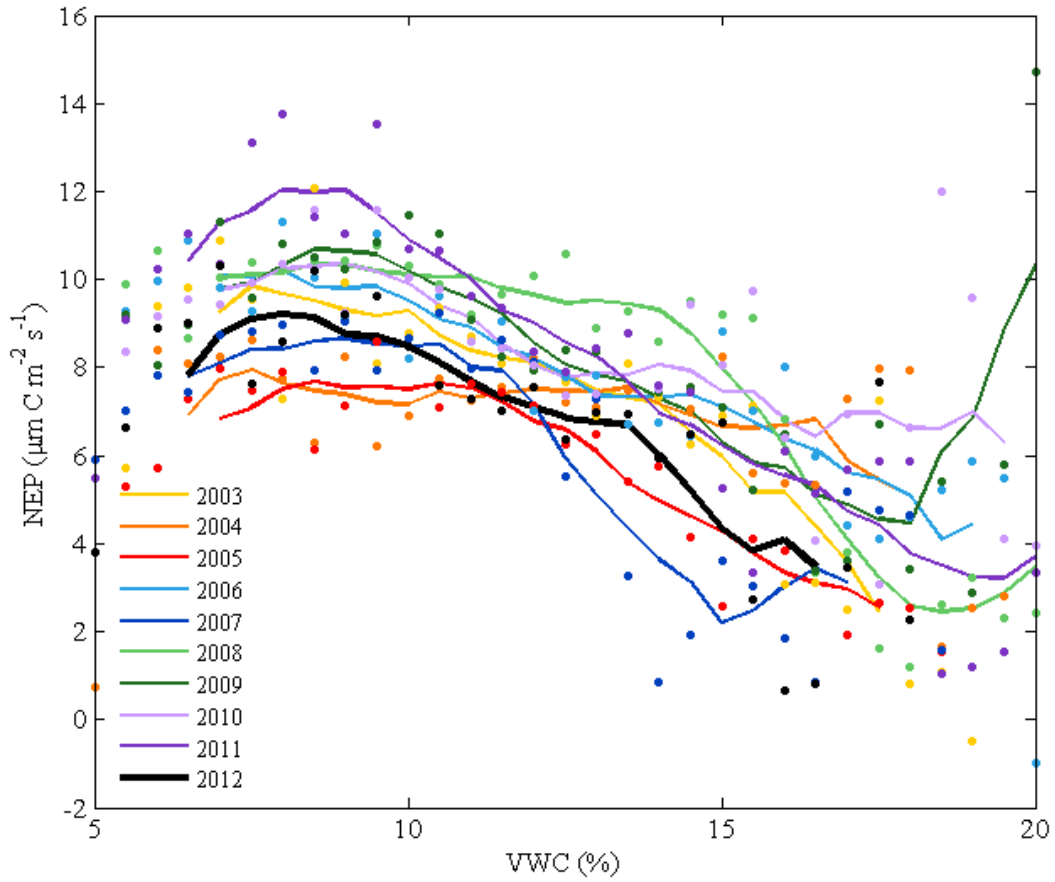
Figure 15. Relationship between daytime growing season measurements of binned volumetric soil water content (VWC, bin size of 0.05%) and non-gapfilled net ecosystem productivity (NEP, μm C m^{-2} second^{-1}). Solid lines show the moving average for each year. The stand was thinned in winter 2012.
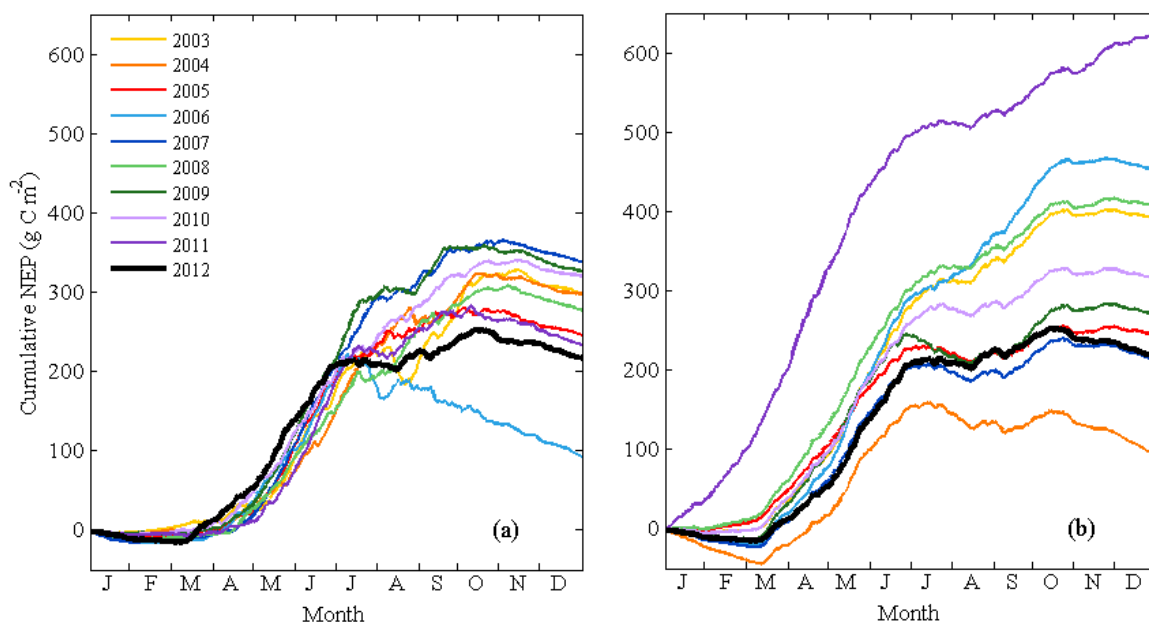
**Figure 16.** Modeled cumulative net ecosystem productivity (NEP, g C m⁻²) at the 74-year old site (TP39). In (a), the model was run using 2012 model parameters against 10 years (2003–2012) of meteorological data. In (b), the same model was run using 10 years (2003–2012) of model parameters against 2012 meteorological data. Line specifications (colour and style) indicate meteorological data year (a) and model parameter year (b). The stand was thinned in winter 2012.
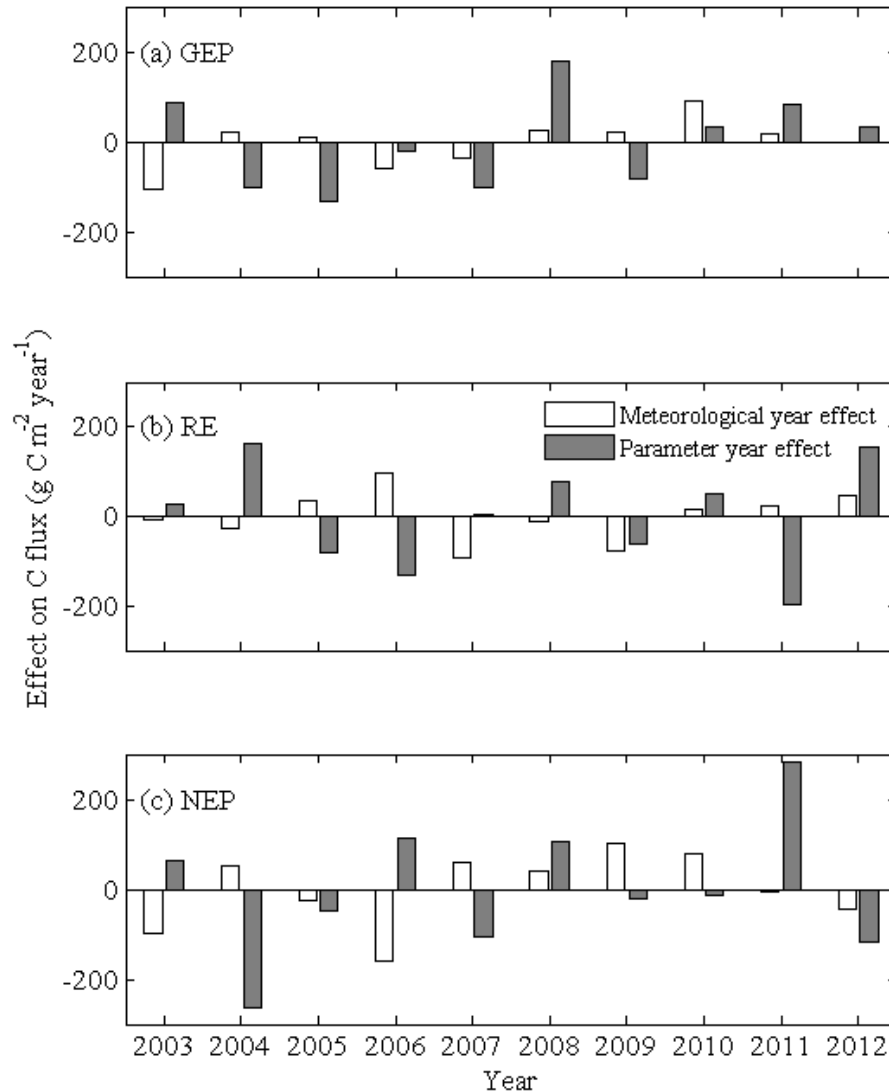
Figure 17. Effects of interannual variability in meteorological conditions ('meteorological year' effects) and model parameters ('parameter year' effects) on modeled CO_2 fluxes (g C m^{-2} $year^{-1}$) at the annual time step: (a) gross ecosystem productivity (GEP), (b) ecosystem respiration (RE), (c) net ecosystem productivity (NEP). A positive effect for RE means increased respiratory losses resulting in a higher rate of respiration, whereas a negative effect for GEP means decreased canopy uptake. The stand was thinned in winter 2012.

APPENDIX A: EDDY COVARIANCE DATA PROCESSING

Processes applied to the calculated half-hourly fluxes, in order of operation, were: (1) outlier and spike removal; (2) footprint filtering; (3) friction velocity (u_*) threshold filtering; (4) RE gap-filling; (5) partitioning of NEE into GEP; (6) GEP gap-filling; and, (7) filling of NEP gaps resulting from instrument malfunction, power outages, calibration or data processing. With the exception of storage calculations, all of these processes were run separately for pre- and post-thinning periods (2003-2011 and 2012, respectively) to avoid confounding effects caused by any phenological changes in the stand resulting from thinning.

Outlier and spike removal

Spikes and outliers in half-hourly NEE measurements, caused by changes in turbulence and water drops on the sonic anemometer, were identified and removed following Papale et al. (2006). First, the acceptability of instances with large differences before and after a spike was evaluated using pre-determined upper and lower thresholds (Papale et al. 2006). Next, an ensemble method was applied which divided data into temporal windows and compared half-hourly values to the calculated mean temporal window value, rejecting points that were significantly different from the mean over the temporal period. On average, 13% of half-hourly NEE measurements were either unavailable due to operational failures and maintenance, or removed during the outlier and spike removal process.

Footprint model

TP39 is surrounded by similar-aged stands of different species, predominantly red pine. Because the objective of this study was to evaluate thinning effects on carbon dynamics, it was necessary to include only flux measurements from within the boundary of the white pine stand by excluding adjacent stands of other species (Aubinet et al. 311). To do this, a one-dimensional analytical footprint model was applied following Kljun et al. (2004). This model was developed from parameterization of a previously described Lagrangian stochastic dispersion model (Kljun et al. 2002). An acceptance level of 80% was used, meaning that for each half-hourly measurement to be retained, at least 80% of the flux must have been estimated to come from within the source area. Half-hourly values were discarded if less than 80% of the measured flux came from within the source area. For a detailed explanation of the footprint method selection for this site, see Brodeur (2013). On average, 46% of half-hourly NEE measurements were removed each year by the footprint filter.

Turbulence correction

To correct for the underestimation of nighttime fluxes due to low turbulence, which results in a selective systematic error, a u_* threshold (u_{*th}) was applied to nighttime data to remove fluxes measured during periods of insufficient turbulence (Aubinet et al. 2000). A modification of the u_{*th} methods presented in Reichstein et al. (2005) and Barr et al. (2012) was applied. For each three month interval, nighttime data were selected and divided into six equally-sized temperature classes, then further sub-divided into twenty equally-sized u_* classes (Reichstein et al. 2005). For each temperature class, the threshold was defined as

the u_* class in which the average nighttime flux reached more than 99% of the average flux at the higher u_* classes. The threshold was rejected if the temperature class, temperature and u_* were correlated ($|r| \geq 0.4$) (Reichstein et al. 2005). Bootstrapping was used to run each season 100 times, resulting in 100 seasonal values per year (Brodeur 2013). The median of these seasonal values was chosen as the annual u_{*th}. Half-hourly nighttime fluxes were discarded if the calculated u_* was lower than the annual u_{*th}. Annual u_{*th} values for the study period are given in Table 4. On average, 28% of half-hourly measurements of NEE were removed each year by the u_{*th}.

Table 4. Annual friction velocity (u_*) thresholds.

	2003	2004	2005	2006	2007	2008	2009	2010	2011	2012
Annual u_{*th} (m s^{-1})	0.41	0.41	0.41	0.38	0.45	0.47	0.45	0.51	0.46	0.47

Table 5 shows the percentage of data removed during each step of EC data processing for the study period. On average, 87% of half-hourly measurements of NEE were gap-filled.

Table 5. Percentage of data removed during each step of EC data processing.

	2003	2004	2005	2006	2007	2008	2009	2010	2011	2012
Percent removed due to operations, calibrations, spikes and outliers	30.6	20.7	9.5	6.3	8.6	11.0	13.9	9.4	11.6	7.6
Percent removed by u_{*th}	22.7	23.7	29.7	26.4	29.7	29.5	27.2	30.7	26.9	30.4
Percent removed by footprint	35.8	44.6	52.0	47.5	47.8	43.0	46.9	52.0	49.6	48.6
Total percent removed	89.1	89.0	91.2	80.3	86.1	83.5	88.0	92.2	88.1	86.6

Eddy covariance gap-filling and partitioning

It is assumed that when photosynthesis is not occurring, at night and when Ta is less than 2°C, measured NEE equals RE. Remaining gaps in half-hourly RE were filled using a non-linear regression-type method introduced by Richardson et al. (2007) and adapted for

this site in Peichl et al. (2010a) and Brodeur (2013). RE is modeled as a function of Ts and

VWC in the rooting zone (VWC_{30}), following Equation 1:

$$RE = R_{10} \times Q_{10}^{\frac{(Ts-10)}{10}} \times f(VWC_{30}) \tag{1}$$

where R_{10} and Q_{10} are temperature response parameters that explain the relationship

between RE and Ts, and $f(VWC_{30})$ is a sigmoidal function that characterizes the role of

VWC_{30} in modifying the temperature response of RE as:

$$f(x) = \frac{1}{[1+\exp(c_1 - c_2 x)]} \tag{2}$$

where c_1 and c_2 are parameters ranging between 0 and 1 as a function of VWC_{30}. This acts

as a scaling function for the RE-Ts relationship. For a detailed explanation of this

methodology, see Brodeur (2013).

GEP was estimated by subtracting NEE from gap-filled RE. During nighttime and

when Ta was less than 2°C, GEP was set to zero. When either NEE or RE was unavailable,

GEP was modeled using the following relationship:

$$GEP = \frac{\alpha PPFD \beta}{\alpha PPFD + \beta} \times f(Ts) \times f(VPD) \times f(VWC_{30}) \tag{3}$$

where PPFD is downward photosynthetic photon flux density (μmol m^{-2} s^{-1}), α is the quantum yield and β is photosynthetic capacity (Peichl et al. 2010a; Brodeur 2013). The first term in Equation 4 is a rectangular hyperbola relationship between GEP and PAR, and the remaining terms describe sigmoidal-type scaling responses of GEP to Ts, VPD and VWC$_{30}$, respectively.

Once gaps in RE and GEP were filled, remaining gaps in NEE resulting from instrument malfunctions, power outages, calibration and data processing were filled using the difference between modeled GEP and RE. Net ecosystem productivity (NEP) was calculated as negative NEE.

APPENDIX B: GAP-FILLING COEFFICIENTS

Table 6. Model coefficients for the relationship between ecosystem respiration (RE μm C m^{-2} second^{-1}) and soil temperature (Ts, °C).

	RE Model Coefficients	
2003	2.02	4.27
2004	2.73	3.20
2005	2.19	3.23
2006	2.31	3.34
2007	2.22	3.25
2008	2.71	3.37
2009	2.41	3.35
2010	2.29	3.42
2011	2.19	2.86
2012	2.51	3.28

Table 7. Model coefficients for the relationship between gross ecosystem productivity (GEP, μm C m^{-2} second^{-1}) and photosynthetically active radiation (PAR, μmol m^{-2} second^{-1}).

	GEP Model Coefficients	
2003	0.07	51.59
2004	0.09	77.92
2005	0.06	68.85
2006	0.05	25.98
2007	0.07	72.38
2008	0.10	76.52
2009	0.06	67.72
2010	0.09	83.42
2011	0.05	52.09
2012	0.07	55.73